A DETAILED STUDY OF THE PHYSICAL PROPERTIES OF RECENTLY DEPOSITED SEDIMENTS FROM A MINIBASIN, NORTHWEST GULF OF MEXICO

A Thesis

by

MARCO ANTONIO SANTOS CASTANEDA

Submitted to the Office of Graduate Studies of
Texas A&M University
in partial fulfillment of the requirements for the degree of

MASTER OF SCIENCE

May 2012

Major Subject: Oceanography

A DETAILED STUDY OF THE PHYSICAL PROPERTIES OF RECENTLY DEPOSITED SEDIMENTS FROM A MINIBASIN, NORTHWEST GULF OF MEXICO

A Thesis

by

MARCO ANTONIO SANTOS CASTANEDA

Submitted to the Office of Graduate Studies of
Texas A&M University
in partial fulfillment of the requirements for the degree of

MASTER OF SCIENCE

Approved by:

Co-Chairs of Committee,	Niall Slowey
	William Bryant
Committee Member,	Zenon Medina-Cetina
Head of Department,	Piers Chapman

May 2012

Major Subject: Oceanography

ABSTRACT

A Detailed Study of the Physical Properties of Recently Deposited Sediments from a Minibasin, Northwest Gulf of Mexico. (May 2012)

Marco Antonio Santos Castaneda, B.S., Universidad Naval Comandante Rafael Moran Valverde

Co-Chairs of Advisory Committee: Dr. Niall Slowey
Dr. William Bryant

High-resolution seismic data from lower slope basins in the vicinity of Bryant and Keathley Canyons suggest the recent occurrence of thin mud flow events which influence the physical properties of the shallow sediments of the minibasin. Therefore to understand the effect of these events on the physical properties, a very high spatial resolution investigation of the following properties was undertaken: bulk density, grain density, shear strength, water content, “calcium carbonate” content, compressional wave velocity, and the relative elemental composition, of the first 5 meters of the seabed sediments.

The availability of the sediment cores JPC-29 and JPC-36, recovered from either side of a lower slope minibasin, provided the undisturbed sections of marine sediments to measure these properties. We used the multisensor core logger, miniature vane, fall cone, pycnometer, coulometer and X-ray fluorescence scanner in a very high sampling resolution, to accurately measure the variations of the properties with depth. We compared values of the same

property obtained by independent techniques, determined the relationships among the properties, investigated how the properties vary with depth in the two cores, and examined how sampling resolution influenced the expression of features in downcore profiles of the properties.

The results of this research demonstrated that the Multisensor Core Logger (MSCL) is an efficient method to calculate the bulk density of the marine sediments; the fall cone and the mini vane test were consistent in their results. Sediment water content and bulk density showed an inverse relationship. When there is a variety in grain sizes and types, there is less pore space which can be occupied by seawater and greater contact between grains resulting in high shear strength. The downcore profiles of properties showed that bulk density and shear strength generally increase with depth, while water content and “calcium carbonate” content decrease with depth. Two interesting features of high bulk density were explained through the interrelationships that exist among physical properties. Finally, sampling resolution is important because it affects how actual variations in the seabed’s characteristics are resolved in physical property data, so appropriate sampling resolution must be selected based upon the specific research objectives that need to be addressed.

DEDICATION

To my family.

ACKNOWLEDGEMENTS

I would like to thank my committee co-chair, Dr. Slowey, for the guidance, friendship and unconditional support, co-chair, Dr. William Bryant, for his thoughtful advice and my committee member, Dr. Medina-Cetina, for the help throughout the course of this research.

Thanks to my friends and colleagues for the comradeship during my two years at Texas A&M University.

Thanks to Dr. Mitch Lyle, Adrian Miner, Elda Ramirez, Cassie Rutherford, Julia Shackford, Teddy Them, and Alan Young for their support and help with the research.

Thanks to SENECYT, the Ecuadorian Navy, and the Department of Oceanography at Texas A&M University.

Finally thanks to my family for being always beside me.

TABLE OF CONTENTS

LIST OF FIGURES

Page

1. INTRODUCTION

The continental slope of the northwest Gulf of Mexico is covered by a thick section of late Quaternary-aged hemipelagic sediments. The fundamental physical properties of these sediments reflect the combined influence of depositional and erosional processes active at the seafloor (e.g., Knebes and Carson,1979; Schlager and Camber, 1986; Masson 1999; Twichell 2011), the occurrence of mass wasting events (e.g., Booth 1979; Kenyon 1987; Lowrie et al, 2004; Silva et al, 2004; Tappin et al, 2010; Baeten et al, 2011), and the structural evolution of the slope (e.g., Kastens and Shor, 1985; Bryant et al, 1991; Mallarino et al, 2006; Combellas and Galoway, 2006; Konyukhov 2008). Variations of sediment properties preserve valuable records of the influence of these environmental processes at specific sites on the slope as well as the history and regional effects of glacial-interglacial changes climate (e.g., Flower et al, 2004; Dezileau et al, 2007; Mahiques et al, 2007; Meckler et al, 2008; Ingram et al, 2010) and sea level (e.g., Posamentier and Walker, 2006; Mallarino et al, 2006; Kaiyu 2009; Rodrigues et al, 2010; Duchamp-Alphonse et al, 2011). Of great practical importance for both engineering and geological applications associated with oil production, sediment property variations exert strong control on the bearing capacity, slope stability, determine the origin of reflectors seen on seismic profiles (e.g., Kim and Kim, 2001; Sager et al, 2003; Finkl et al, 2006; Alves 2010; Kilhams et al, 2011), and other important

This thesis follows the style of Geo-Marine Letters.

geotechnical aspects of the seabed (e.g., Bradshaw et al, 2000; Morton 2008; Urgeles et al, 2010; Lee et al,2011; Gay et al, 2011). To address both marine geotechnical and geological issues in the northwest Gulf of Mexico, it is essential to understand the fundamental physical properties of slope sediments.

Two fundamental properties that are frequently studied in investigations of slope sediments are their shear strength and bulk density. The need to determine how these properties vary with depth in the seabed has motivated several groups to study them from the perspective of both marine geology (e.g., Moore, 1962; Kenter and Schlager, 1989; Silva et al., 2004) and geotechnical engineering (Skempton, 1953; Richards and Keller, 1967; Keller and R. Bennett, 1970; Francisca et al., 2005). For such studies, cores of sediment extracted from the seafloor are a valuable source of information. When the seabed is sampled in this way, sediment is available for analysis in the laboratory setting where it is possible to measure multiple physical properties and relate them directly to the lithologic characteristics of the area where the core was obtained. The results of such integrated analysis lead to a better understanding of the sediment configuration and geotechnical characteristics of the seafloor.

High-resolution seismic data from various lower slope basins in the vicinity of Bryant Canyon suggest that thin mudflow and debris flow events may affect the upper portion of the seabed (e.g. Silva et al., 2004; Tripsanas, 2003). We therefore sought to examine undisturbed portions of the seabed to better

characterize the inherent physical properties of the sediment related to slope stability. The availability of two cores collected from the lower slope of the northwest Gulf of Mexico in the vicinity of Bryant and Keathley Canyons offered an opportunity to do this.

This thesis will present the results of an investigation of the sediments in these cores in which the following properties will be determined in very high spatial resolution (more than is customary): bulk density, grain density, shear strength, water content, “calcium carbonate” content, compressional wave velocity, and the relative elemental composition in the sediments. There are several goals: (1) investigate how the properties vary with depth in the two cores, (2) compare values of the same property obtained by independent techniques, (3) determine the relationships among the properties, and (4) examine how sampling resolution influences the expression of features in downcore profiles of the properties. The results will be useful information that may give a better understanding of the sediment morphology in the basin.

2. SITE AND SEDIMENT CORES STUDIED

The Texas-Louisiana Slope is approximately 550-600 km long with water depths between 200 to 3400 meters (e.g., Bryant et al., 1990). A series of raised banks occur along shelf-slope boundary and numerous basins separated by ridges occur along the middle and lower slope. These physiographic features were formed by the upward and lateral movement of allochthonous salt within the seabed (Gealy, 1955). The source of this salt is the Louann Salt and other salt bodies that were originally deposited as the Gulf of Mexico opened during the Late Triassic and the Early to Middle Jurassic periods over 160 million years ago, and then covered by thick sequences of hemipelagic sediments (Salvador, 1986).

The sediment cores to be used for the thesis research proposed here come from the southeastern section of the lower slope of the northwest Gulf of Mexico in the vicinity of Bryant and Keathley Canyons (Figure 1).

The minibasin is about 8 km wide and 6 km long and located at depths of 1,800 to 1,900 meters below sea level (Figure 2). Because the minibasin is near to Bryant Canyon, the seabed of the minibasin must have been strongly influenced by the canyon's sedimentary processes.

The Bryant Canyon is an erosion-deposition river-sourced system that extends from the upper to the lower continental slope. Its morphology and the character of the seafloor sediments on it reflect the combined effects of allochthonous salt movement and downslope sediment transport processes.

Large amounts of riverine sediments reached the upper slope during Plio-Pleistocene glacial lowstands of sea level, then sediment gravity flows transported the sediment down across the slope and deposited thick, dense sediment sequences in the canyon and surrounding minibasins (e.g., Bouma, 1983; Lee et al., 1996). In response to this loading, salt within the seabed migrated laterally from beneath the canyon axis and basins to adjacent areas of the slope, enhancing the bathymetric relief of these features (e.g., Bouma, 1983; Lee et al., 1996). The canyon became inactive and hemipelagic sediment deposition dominated the system during Pleistocene highstands of sea level (Lee et al., 1996). Over this entire time, sediment input decreased because the location of the large Mississippi River system delta started to shift eastwards to its present location (e.g. Tripsanas, 2003).

The research proposed for this thesis will focus on sediments in the upper five meters of cores KMB JPC 29 and KMB JPC 36 from the minibasin. Based on studies of cores from Bryant Canyon reported by Tripsanas et al. (2006; 2007), sediments in the upper five meters of cores JPC 29 and JPC 36 may correspond to the Marine Isotope Stages[1] (MIS) 1 and 2 and probably MIS 3 at the bottom of those sections.

[1] Marine Isotope Stage (MIS) nomenclature as defined by Emiliani (1955, 1966) and Shackleton and Opdyke (1973) refers to prominent variations in the ratio of ^{18}O to ^{16}O in $CaCO_3$ foraminifera shells found in the marine sediments, which reflect the complementary effects of changes in the temperature and the oxygen isotopic composition of seawater that occur during Quaternary glacial-interglacial climate cycles. Odd MIS numbers correspond to periods of warm interglacial climate when sea level is high; even MIS numbers correspond to periods of cool glacial when sea level is low.

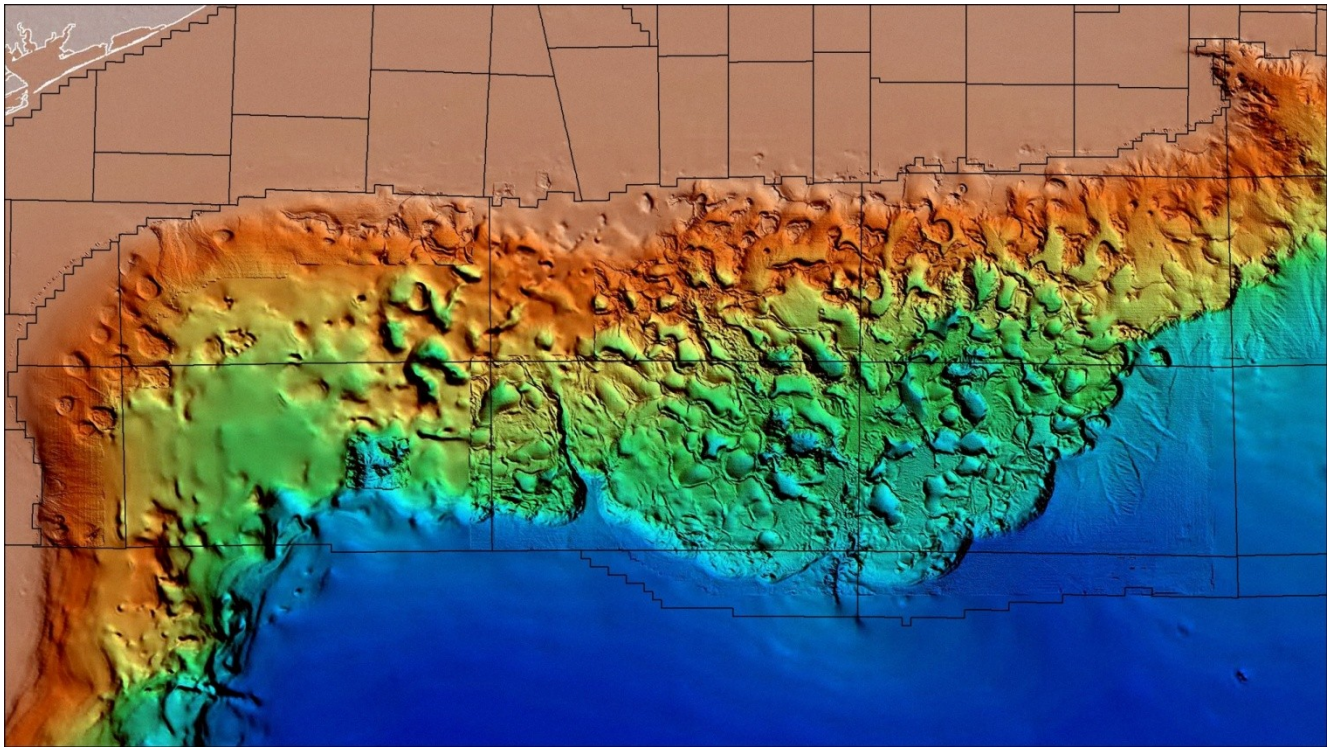

Figure 1 General location of lower slope minibasins in the Bryant and Keathley Canyon areas. Graphic produced using the Sigsbee Slope Basin and Mississipi Canyon bathymetric data (100m Resolution) available from the NOAA and National Geophysical Data Center in GeoMapApp (Ryan et al., 2009).

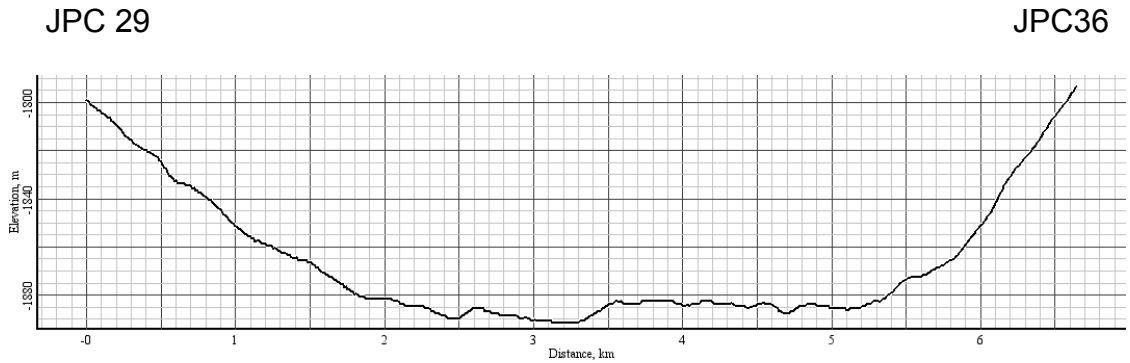

Figure 2 Positions of cores JPC 29 and JPC 36 on a cross section profile of the minibasin that shows the seafloor relief between the cores. Graphic produced using the Sigsbee Slope Basin and Mississipi Canyon bathymetric data (100m Resolution) available from the NOAA and National Geophysical Data Center in GeoMapApp (Ryan et al., 2009)

Sea level varied by about 120 m during the most recent glacial-interglacial cycle (e.g., Fairbanks, 1989, Waelbroeck et al., 2002). Tripsanas et al. (2006, 2007) studied how slope sedimentation in the vicinity of Bryant Canyon changed in conjunction with these sea level variations. When sea level fell at the end of MIS 3 (about 60,000 years ago) and rivers discharged sediment directly onto the upper slope, low density turbidity flows brought sediments to the continental slope in the vicinity of the canyon. At the maximum extent of continental glaciation / lowstand of sea level during the MIS 2 (about 24,000 to 20,000 years ago), the influx of riverine sediments to the upper continental slope and subsequent gravity flows down the canyon continued (e.g., Lee et al., 1996; Tripsanas et al., 2007). The melting of the continental ice sheet at the end MIS 2 and beginning of MIS 1 (about 18,000 to 5,000 years ago) caused a large rise of sea level (e.g., Fairbanks, 1989). The influx of riverine sediments to the slope in the vicinity of Bryant Canyon decreased and hemipelagic sedimentation occurred to the present time (e.g., Tripsanas et al., 2007).

Cores JPC 29 and JPC 36 were recovered using a 4-inch (10-cm) inner diameter piston core. The cores come from opposite sides of the minibasin and the distance between cores is 6.6 km. When they were recovered onto the ship, the cores were immediately cut into sections with lengths of about 3 ft (0.91 m) each and the ends of the sections were capped and sealed. The core sections were returned to College Station and stored upright until they were analyzed in the laboratory. The upper 5 sections of these cores, which contained sediments

from about the uppermost 5 m of the seabed, were kindly made available for the research proposed.

3. METHODS

The upper 5 sections of the cores JPC 29 and JPC 36 contain unconsolidated soft, fine-grained sediments with high moisture content. The methods selected to measure the physical properties are suitable for this type of marine sediment.

Whole core sections were first analyzed using the multisensor core logger to measure the bulk density, water content, and compressional wave velocity of the sediments. Then the core sections were split longitudinally into halves in order to proceed with the measurement of other physical properties. We used the miniature vane and fall cone tests to measure the shear strength; then samples were taken to measure the bulk density of the sediments using the pycnometer, and “calcium carbonate” content with the coulometer. Finally the other half was photographed and used to measure the elemental composition though a X-ray fluorescence scanner.

To avoid alterations in the sediments’ characteristics due to the loss of moisture, the half core sections of sediment were covered with plastic wrap and sealed immediately after they were split, and then stored under high-humidity refrigerated conditions. Just prior to proceeding with the measurements, the sealed half-core sections were equilibrated to ambienct laboratory temperature. Both of the shear strength measurement techniques were performed in rapid succession on the same day, followed immediately by the removal of discrete sediment samples for other analyses. During these procedures, the portions of sediment that were not being measured/sampled were kept covered with plastic.

3.1. Multisensor Core Logger (MSCL)

The MSCL uses Gamma rays and acoustic waves to obtain, in a non-destructive way, important information from the marine sediments.

A transducer emits an acoustic wave in order to measure the P-wave velocity and amplitude of the sound moving across the sediments, this method is described by Shultheiss and McPhail (1989). Meanwhile a scintillation detector senses attenuation of the gamma rays passing through the core's transversal section in order to infer the bulk density, porosity, void ratio and percentage of water content in that specific position (e.g. Boyce, 1976). These measurements were taken every centimeter in order to obtain high resolution profiles of the sediment properties.

3.2. Fall Cone Test

In order to measure the shear strength along the cores, this test was performed every two centimeters over the sediment surface of the working core half, with measurements being offset slight to avoid sediment from one measurement influencing another measurement.

The fall cone test is a geotechnical and engineering method included in the British Standards (BS 1377-2, 1990) (Houlsby, 1982) that is widely used to determine primarily the shear strength of soft sediments (Koumoto and Houlsby, 2001), similar to those found in the upper five meters of the piston cores to be studied.

The device is a simple structure (Figure 3) that allows the cone to fall freely into the sediments and its penetration to be measured very accurately. This distance and cone parameters are used to calculate the shear strength according to the expression derived by Hasbro (1957):

$$\mathrm{Su} = \frac{\mathrm{K}_{60}\mathrm{am}}{\mathrm{d}^2}$$

where *Su* stands for the undrained shear strength measured in kilo Pascal (kPa), *a* is the acceleration of gravity (9.8 m/s^2), *m* is the mass of the cone-rod system in grams, *d* is the cone penetration measured in millimeters, and K_{60} is a constant which depends upon the cone apex angle, which for the present study is 60°.

Various tests have been carried out to define a K value useful to be correlated with other shear strength test for soft sediments, namely the miniature vane test. Wood (1985) obtained a value of 0.29 and Hansbo (1957) a value of 0.24. The latter value seems to produce an underestimation on shear strength and the former results in an overestimation (Lu and Bryant, 1997). Lu and Bryant (1997) suggests a K60 =0.275 as a better estimation to calculate shear strength.

3.3. Miniature Vane Test

The miniature vane test is commonly used to measure shear strength in soft sediments and is considered in the American Society for Testing and Materials (ASTM) as a standard procedure to determine the shear strength on fine-grained sediments (ASTM-D4648-10).

The test apparatus uses a vane blade that is inserted in the sediments and rotated at a constant rate by an electric motor. The vane blade consists of four rectangular blades assembled perpendicularly in a rod; the blades used were 12.7 mm high and 6.35 mm long. The hole created by these blades had dimensions of 12.7 mm for both diameter and height (Figure 4).

A calibrated spring, whose constant spring (k) is known, is incorporated into the system to measure the torque needed to make the sediments fail. The resulting torque reading is used to derive shear strength.

The vane blade is perpendicularly introduced by twice its height into the sediments. Because the blades are very thin, insertion of the vane blade in the sediments doesn't produce a considerable disturbance in sediment properties (ASTM-D4648-10).

An electric motor introduces rotation to the vane blade-spring system at an approximate rate of 90° per minute. The upper part of the spring rotates with the system, while the lower part remains static until the accumulated torque is able to overcome the resistance to movement in the sediments. Once the sediments begin to fail the vane starts to rotate and with it the lower part of the calibrated spring. Finally total failure occurs when the spring transmits enough torque to overcome the shearing resistance of the sediments. The required torque to produce the total failure of the sediments is measured through the angular displacement of the spring deflection. This torque is proportional to the shear strength of the sediment (Holtz et al., 2011).

Figure 3 Picture of the fall cone apparatus.

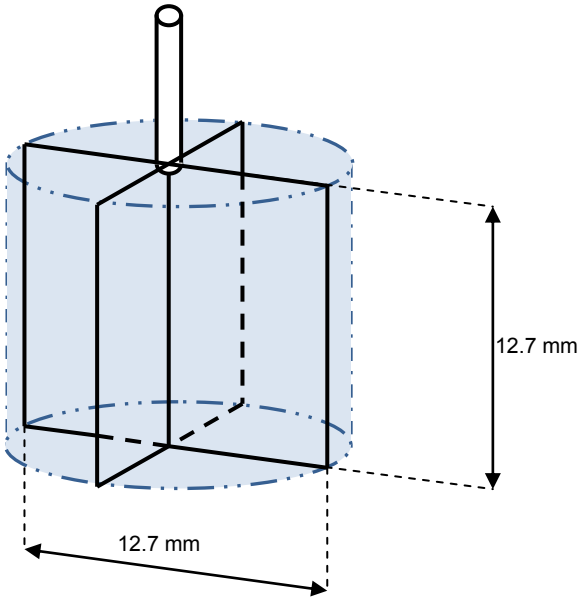

Figure 4 Graph describing the dimensions and the shape of the vane used.

According with the ASTM-D4648-10 procedure to calculate the undrained shear strength we used the formula:

$$\mathrm{Su} = \frac{\mathrm{T}}{\mathrm{K}}$$

where *T* is the torque that results in total failure of the sediments, and *K* is a constant that is function of the blade geometry, which is calculated by:

$$\mathrm{K} = \frac{\pi \mathrm{D}^2 \mathrm{H}}{2 \times 10^9}\left(1 + \frac{\mathrm{D}}{3\mathrm{H}}\right)$$

where *D* is the diameter of the vane blade in millimeters and *H* is the blade height in millimeters. Hence, *K* is 4.29 X 10^{-6} m^3 for the vane blade dimensions previously described. The formulae presented in the ASTM-D4648-10 procedure for this calculation has typo in the denominator, instead of using 10^9 it shows 10^6; this typo is corrected in the formula shown above.

The torque is calculated using the spring constant (*k*) and the spring deflection angle ($\Delta°$) at the instant of total failure, using the relationship:

$$\mathrm{T} = \frac{\Delta°}{k}$$

where the torque obtained is in Newton meters (N m).

Finally, the shear strength can be calculated in Pascal, using a simpler equation:

$$\mathrm{Su} = \frac{\Delta°}{Kk}$$

Through this relation the undrained shear strength is defined as a function of the deflection angle, spring constant, and vane blade constant.

The shear strength test was performed every four centimeters over the sediment surface of the split core sections. The miniature vane test affects a greater volume of sediment than the fall cone test, so if the miniature vane shear test were to be performed every two centimeters, as was done with the fall cone, the perturbation in the sediments caused by the vane would have affected the reading in the next test.

This procedure resulted in another profile of shear strength over depth with less resolution than obtained by the fall cone procedure but extremely important for multi-core correlations.

As soon as the shear strength tests were completed we took two sediment samples and stored them in different vials. One was immediately placed in the scale to define the “total wet weight”, and the other was used in other tests. Sampling was performed every four centimeters at the same place where the mini vane test was performed. This insured that the data obtained from each procedure were compared directly. The samples in which wet weight was known were freeze dried and then weighed again to determine the “total dry weight” of the sample, which is a parameter needed to calculate the sample water content and grain density.

3.4. Pycnometer

A pycnometer was used to determine the volume of the dry samples, a parameter needed to calculate the wet bulk density, dry bulk density, the grain density and water content. The Pycnometer is a proven device used in different

applications to measure the volume of a sample and is considered in the ASTM (ASTM D5550-06).

The vial containing dry sediments were sealed in a compartment whose volume is known. An inert gas (helium) is added to the compartment and then expanded into another chamber. The change in pressure due to expansion is used to define the volume of the sediments collected in the sample. This procedure was repeated by the device five times to obtain accurate results by calculating the standard deviation of these measured volumes. The “average volume” in cm^3 was used in the calculations following the Proceedings of the Ocean Drilling Program (e.g. Dadey et al., 1992; Backman et al., 2006).

Before the collection of the samples took place, all the empty vials were labeled and weighed. This information was used to determine the weight of sediments in each sample for the wet and dry conditions.

The information of vial weight, total wet weight, total dry weight, glass density of the vial and the volume calculated was loaded in a Microsoft Excel spreadsheet to perform further calculations following the Proceedings of the Ocean Drilling Program. We obtained important information like the salt mass, and water content of every sample, its dry bulk density, and grain density. These data resulted in a depth profile for each variable.

The empty vial weight was subtracted from the total wet weight and total dry weight in order to obtain the “wet weight” and “dry weight” respectively. Thus, the “water weight” was obtained from:

$$\text{Water weight (g)} = \text{Wet weight} - \text{Dry weight}$$

Since the pycnometer uses the displacement of gas to calculate volume, temperature variations can introduce errors in the measurements. Therefore, it was necessary to weigh and run a blank vial at least four times per day when sampling in order to obtain the “average blank correction”. This value is the average of the volume obtained from the blank vial from that specific day.

Weighing and running several empty vials in the pycnometer let us average the results and obtain the vial glass density, which was needed in the vial correction.

The vial correction is obtained from:

$$\text{Vial Correction } (\text{cm}^3) = \frac{\text{Blank vial weight} - \text{Vial weight}}{\text{Glass density}}$$

This correction must be incorporated in the average volume calculated to obtain the “corrected solids volume”, which corresponds to the volume of grains and salt of the sample:

$$\begin{matrix}\text{Corrected} \\ \text{solids volume}\end{matrix} \ (\text{cm}^3) = \begin{matrix}\text{Average} \\ \text{volume}\end{matrix} + \begin{matrix}\text{Average} \\ \text{blank correction}\end{matrix} + \begin{matrix}\text{Vial} \\ \text{correction}\end{matrix}$$

With the correction made to the grain and salt volume we can obtain its density:

$$\text{Grain + salt density} = \frac{\text{Dry weight}}{\text{Corrected solids volume}}$$

Despite the allochthonous salt beneath the seabed in the Gulf of Mexico, high salinity pore water presents high values (over 100 g /l) in sediments below 2 km under the seafloor (Hanor and Mercer, 2009). Therefore, the pore water salinity in the shallow sediments is not affected and can be considered as a normal salinity of 35 ‰ (Dadey et al., 1992).

$$\text{Mass salt (g)} = 0.0351 \times \text{Water weight}$$

According to Takahashi (2011), the sea water salt density was considered to be 2.22 g/cm^3.

$$\text{Volume salt (cm}^3\text{)} = \frac{\text{Mass salt}}{2.22 \frac{\text{g}}{\text{cm}^3}}$$

The “grain mass” was obtained by subtracting the amount of salt in the sample from its weight. The same principle was applied to obtain the “grain volume”:

$$\text{Grain mass} = \text{Dry weight} - \text{Mass salt}$$

$$\text{Grain volume} = \text{Corrected solids volume} - \text{Salt volume}$$

The wet weight is already known, and to obtain the “wet bulk density” it was necessary to determine the volume of sediments before being freeze dried, which was called “total volume”. Water volume was obtained from the water mass in the sample and the water density (1 g/cm^3):

$$\text{Total volume} = \text{Corrected grain} + \text{Salt volume} + \text{Water volume}$$

$$\text{Wet bulk density} = \frac{\text{Wet weight}}{\text{Total volume}}$$

With the information calculated we were able to determine the “Dry bulk density” and the “Grain density”:

$$\text{Dry bulk Density} = \frac{\text{Grain mass}}{\text{Total volume}}$$

$$\text{Grain density} = \frac{\text{Wet weight}}{\text{Grain volume}}$$

Finally the water content was calculated using the wet weight and including the salt that was dissolved in it:

$$\text{Water content}(\%) = \frac{\text{Water weight} + \text{Mass Salt}}{\text{Wet weight}} \times 100\%$$

3.5. Coulometer

The carbon content in the samples was determined by a coulometer. Approximately 20 mg of dry sediments were introduced in a vial and sealed. Phosphoric acid was injected into the sealed vial and the reaction evolves “carbon dioxide” gas that was directed to the coulometer cell.

The coulometer cell was filled in the cathode with 100mL of “carbon cathode” solution, the anode with ¼” of potassium iodide and “carbon anode” solution. A top with a platinum electrode and a tube destined to conduct the “carbon dioxide” produced seals the cathode, while the silver anode was sealed with another top. Once the cell was placed in the coulometer and the wires and tube were attached in the proper position, the coulometer was turned on and in a few minutes the solution became blue and was ready to use.

The “carbon dioxide” that went into the coulometer cell decreased the

alkalinity of the solution. The solution returned to the original alkalinity after an electric current was introduced. The electric charge, measured in coulombs, used in this process is proportional to the volume of “carbon dioxide” absorbed.

The “carbon dioxide” measured was directly related to the amount of “calcium carbonate”. This value was used to calculate the percentage of “calcium carbonate” in the sediment.

3.6. X-Ray Fluorescence Scanner (XRF)

This is a non destructive test that was performed on the split core side that was not used in the shear strength tests and showed the relative elemental composition in the sediments.

X-ray radiation was emitted over the sediments and resulted in excitation of the electrons, which changed energy states as a response. The distinct response of the elements was recorded and led us to estimate elemental abundance within the core (Rothwell and Rack, 2006). For the present study, the XRF Scanner was set to extract information every centimeter, obtaining high resolution profiles of elemental composition of the sediments down core.

4. DATA ANALYSIS

4.1. Variation of Properties with Depth

The ways that the physical properties of the sediments vary with depth in the seabed provides important information about both the stability and the geologic history of the seabed. For example, normally we expect that there will be overall trends of increasing bulk density and shear strength as depth increases. While such increases do occur in the upper 5 meters of cores JPC-29 and JPC-36, the data shows some clear deviations from the overall trends. Consistent depth intervals in both cores were identified where one or more physical properties display patterns of variation that reflect fundamental changes in the nature of the sediments (see Figure 5). The characteristic physical properties of each depth interval are described in this section and the reasons for the interrelationships among these properties will be discussed in a subsequent section.

Interval “A” corresponds to the uppermost 190 cm of the seabed. It is characterized by a broad relative maximum in bulk density and the high “calcium carbonate” contents. Over the depth range of 0 to 100 cm, bulk density increases from 1.34 to 1.42 g/cm^3, then bulk density decreases to a minimum value of 1.28 g/cm^3 at approximately 190 cm. This value is the lowest bulk density in bothcores. The pattern of water content variation is the exact inverse of the pattern of bulk density variation, with values decreasing from 61% to 53% in the first 100 cm, then increasing to a maximum of 67% at approximately 190 cm.

The “calcium carbonate” increases from 28% at the top of the cores to 33% at 130 cm, which is the maximum measured value in the cores, then it fall sharply to a minimum of 11.5% at 190 cm. This low “calcium carbonate” content coincides with the very low bulk density. Shear strength decreases slightly from 0 to 60 cm, then increases generally with depth following the shape of the bulk density profile.

Interval “B” spans the depth range of 190 to 300 cm and is marked by coincident, sharp increases in bulk density and shear strength with depth. Bulk density increases from 1.28 g/cm^3 to a maximum of 1.75 g/cm^3 at approximately 280 cm. There are several notable features in interval “B” that exists in both cores JPC-29 and JPC-36. Those are located at about 275 cm depth, there are several closely spaced sediment layers with very high bulk density. These layers are each approximately 4 cm thick and are separated by approximately 2 cm of relatively low-density sediments like those in the upper portion of the depth interval. Water content keeps its decreasing trend with depth and shows an interesting feature of particularly low water content that starts at 267 cm depth and reaches the lowest water content of the cores at 284 cm; 37% and 42% for JPC-29 and JPC-36, respectively. Then the water content increases and at the end of this interval reaches 54% which is a value concordant with the general profile trend for depth intervals B and C.

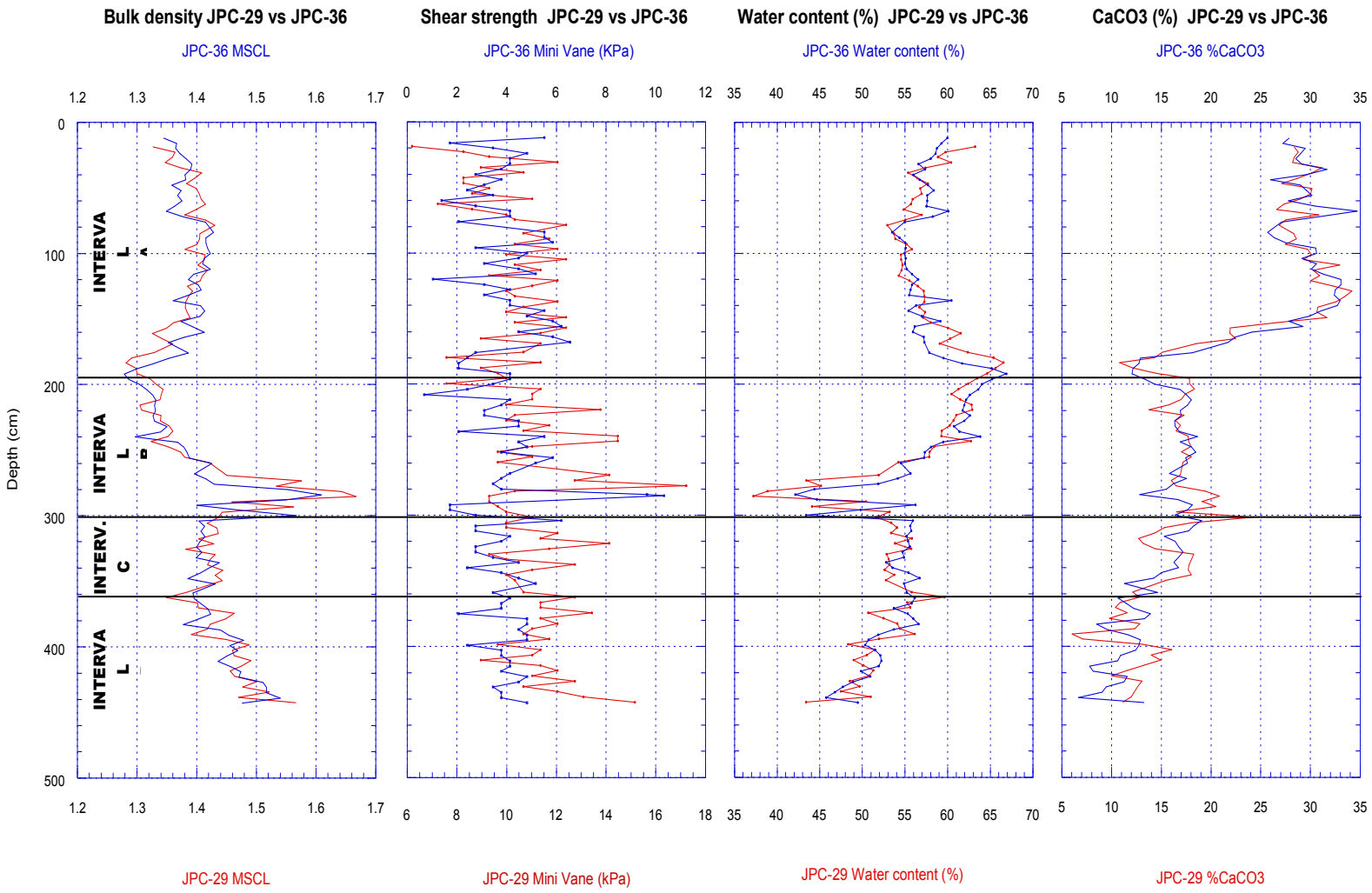

Figure 5 Comparison of bulk density, shear strength, water content and “calcium carbonate” content between JPC-29 and JPC-36 with the visualization of the intervals.

Shear strength increases with depth in interval B with a sharp spike of high shear strength of 17.2 kPa at 277cm depth in JPC-29, and 10.4 kPa at 284 cm depth in JPC-36. These spikes are consistent with the layers of high bulk density founded in this interval.

The biogenic “calcium carbonate” in interval B varies in the range of 16% to 18%, remaining essentially constant until 277 cm depth. Then the “calcium carbonate” content in JPC-29 spikes to 20% at 285 cm, but at the same depth JPC-36 shows 13% “calcium carbonate” content, which is a low spike in the profile. This behavior difference between the two cores was analyzed using as reference the elemental relative composition of calcium form the XRF. The XRF profile for JPC-29 shows two low spikes while the “calcium carbonate” profile at that depth just shows one. The profiles obtained from the XRF are able to resolve features that the “calcium carbonate” content can’t due the different sampling resolution (see Figure 6) (this fact is discussed in more detail in a later section). Since the XRF profiles shows the accurate “calcium carbonate” behavior in this layers, we can say that these are low “calcium carbonate” spikes that correspond to sediments of high bulk density and shear strength.

The sediments in depth interval “C” (from 300 cm to 360 cm) have generally uniform physical properties. Bulk density values, which oscillate within the ranges 1.38 g/cm^3 and 1.43 g/cm^3, shear strength increases only slightly with depth, and “calcium carbonate” decreases slightly from 18% to 11% with depth. It is worth noting that a spike of low bulk density does occur at 360 cm in

KMB-29 and 353 cm in KMB-36. This feature is well defined by the MSCL profile and replicated by the pycnometer data in the core KMB-29. The reason why this spike is not consistent with the pycnometer profile in core KMB-36 should be attributed to the coarser sampling resolution of the pycnometer-based measurements relative to the MSCL measurements.

Depth interval “D” is characterized by steady increases of the bulk density and shear strength with depth. Bulk density displays an overall increase of 1.39 g/cm^3 to 1.53 g/cm^3. The “calcium carbonate” content exhibits a very slight decrease from 11% to 10% with depth.

4.2. Physical Properties Values Obtained by Independent Techniques

Several properties of the sediments in cores JPC-29 and JPC-36 were each determined by independent techniques. Values determined using these techniques are compared in this section, providing an opportunity to better understand both the physical significance and limitations of results obtained by each technique.

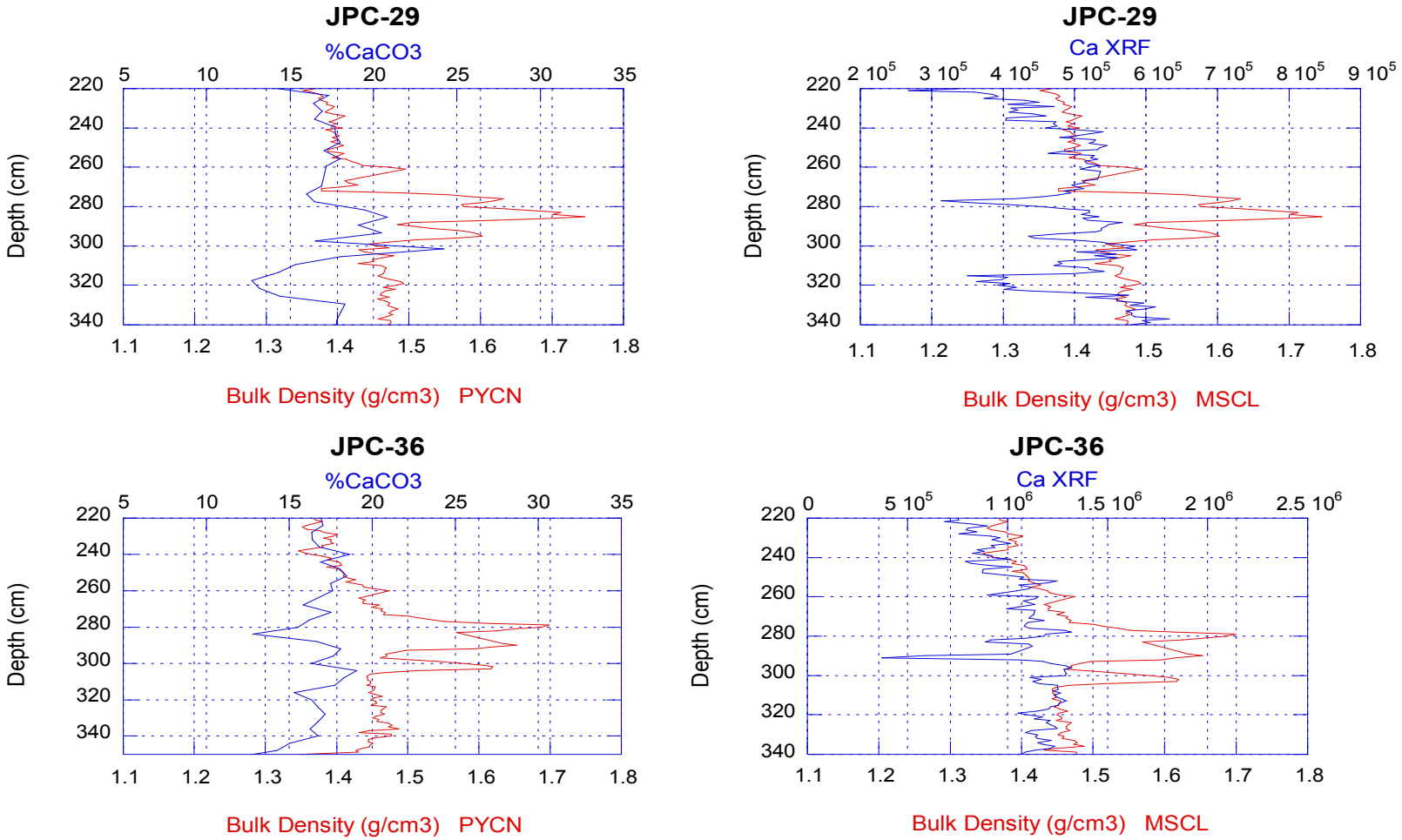

Figure 6 The 4 cm sampling resolution in the $CaCO_3$% profile wasn't able to represent the low spike of "calcium carbonate" content in JPC-29 at 280 cm, which is present in the 1 cm sampling resolution profile of relative Ca content obtained by the XRF. The JPC-36 $CaCO_3$% profile misses one of the two low spikes that the Ca XRF profile shows.

Sediment bulk density was determined two ways. First, the bulk density of sediments in the unopened cores was calculated based upon the MSCL measured extent that the sediments attenuated gamma rays. Second, the bulk density of discrete sediment samples taken from the cores were calculated based upon their water content and grain density under the assumption that the sediments were saturated with seawater. The water content and grain density were measured by weighing the samples before and after drying, and using the pycnometer to determine grain volume. It was not possible to make bulk density measurements at exactly the same depths in the cores using these two different techniques, so MSCL based values were interpolated to obtain estimated values at the same depths where discrete samples were taken.

Figure 7 and Figure 8 show that profiles of bulk density versus depth obtained from cores JPC-29 and JPC-36 using the two techniques display very similar patterns of variability, including the high bulk density spikes that occur in the lower portion of depth interval B (270 to 300 cm). A direct comparison of the bulk density values in Figure 9 confirms this close correspondence with R = 0.96 for 200 points and indicates techniques show similar ranges in values. The MSCL based values generally did exceed discrete sample based values by 0.04 g/cm^3. This small difference may result from the MSCL assuming a constant grain density along the core.

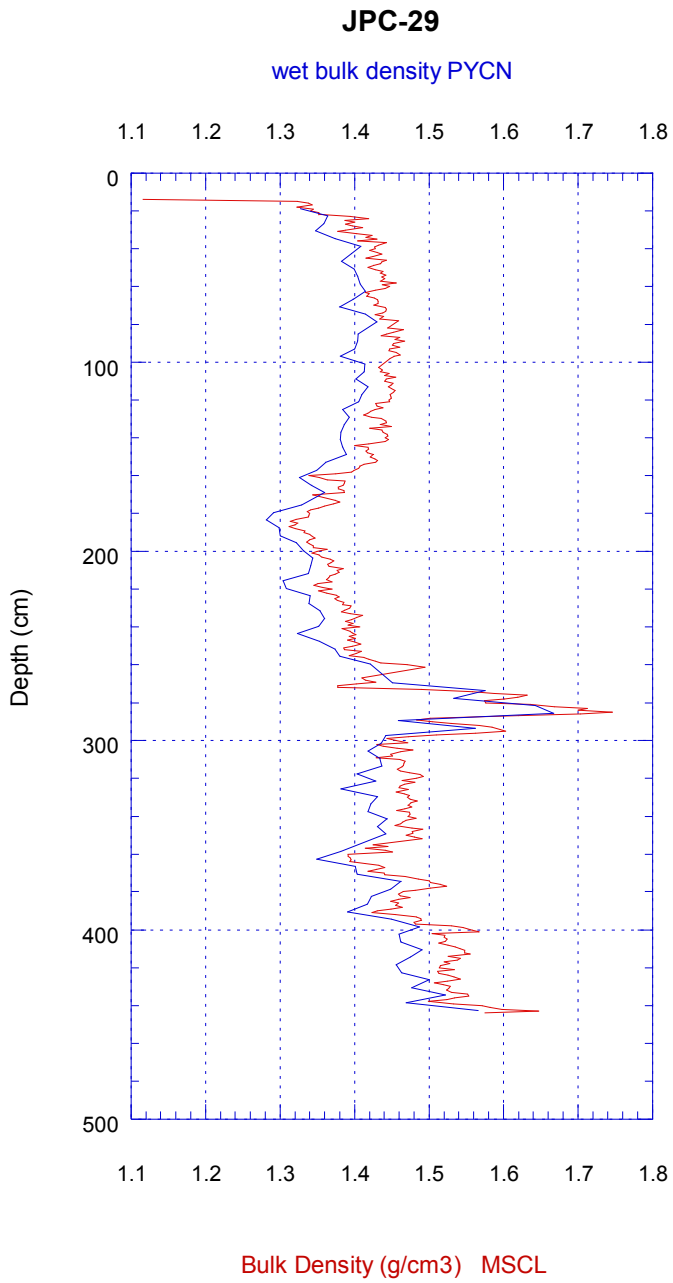

Figure 7 Comparison of bulk density profiles obtained by the MSCL and pycnometer for JPC-29.

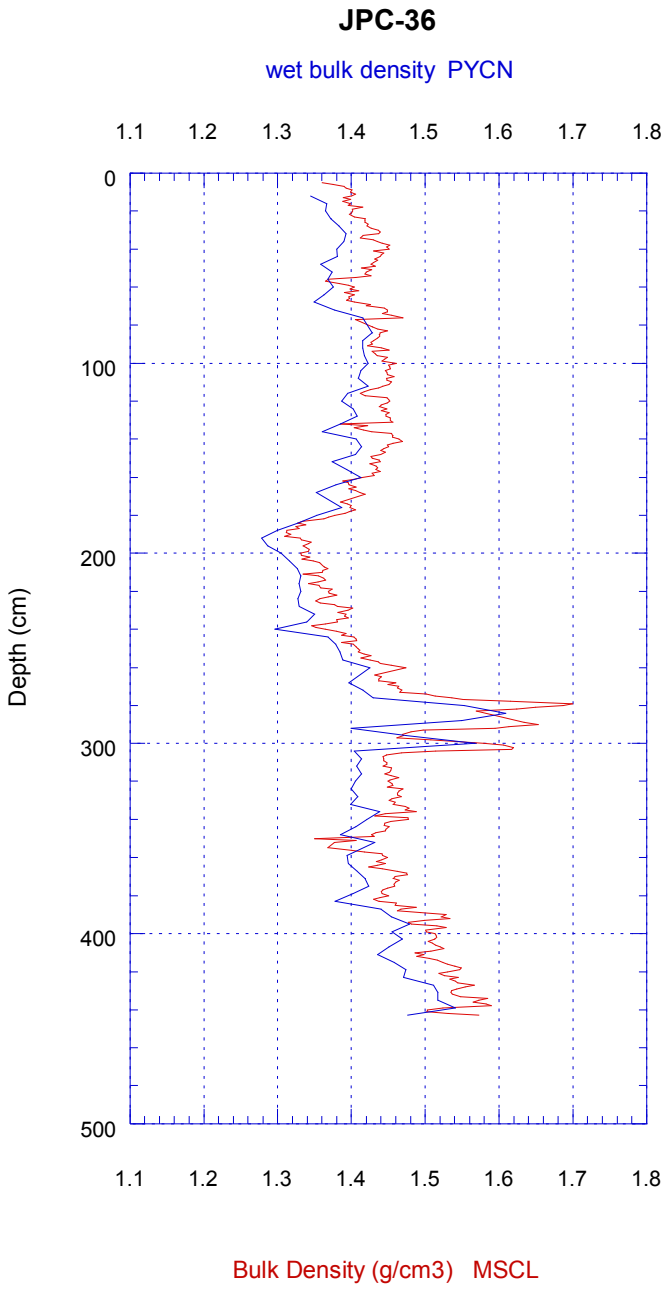

Figure 8 Comparison of bulk density profiles obtained by the MSCL and pycnometer for JPC-36.

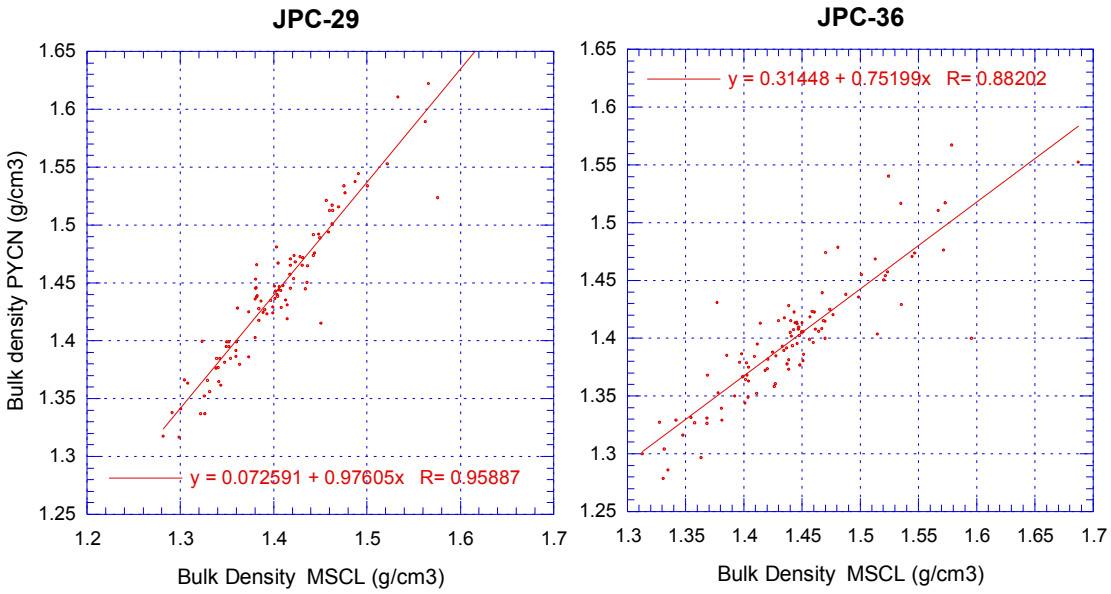

Figure 9 Comparison of bulk density values obtained by independent methods demonstrate its close correlation.

Sediment shear strength was assessed two ways. The miniature vane technique measures the capability of the sediments to bear stress in a cylindrical volume of sediments, and the fall cone technique measures the capability of the sediment to resist penetration.

The miniature vane technique is commonly used in the marine geotechnical field and the values obtained here are consistent to those presented in other studies of the same area (e.g. Silva et al., 2004). In contrast, the fall cone technique is seldom employed in investigations of Gulf of Mexico sediments and a fall cone coefficient has not yet been established for the marine sediments along the lower slope of the northwestern Gulf of Mexico.

The miniature vane values are therefore used as the reference for the overall behavior of shear strength with depth, while the fall cone values are taken to be a relative measure of shear strength only.

Figure 10 and Figure 11 demonstrate that the profiles of both methods are in general consistent one to other. The shear strength profiles show a slight but constant tendency of shear strength to increase with depth. The maximum value of shear strength is 17.2 kPa, and the minimum 6.2 kPa. The main feature in the cores is one spike of high shear strength, which is consistent in the two profiles, located at 277.5 cm. This spike is clearly replicated in both methods and its values are about 17.2 kPa for JPC-29 and 10.3 kPa for JPC-36.

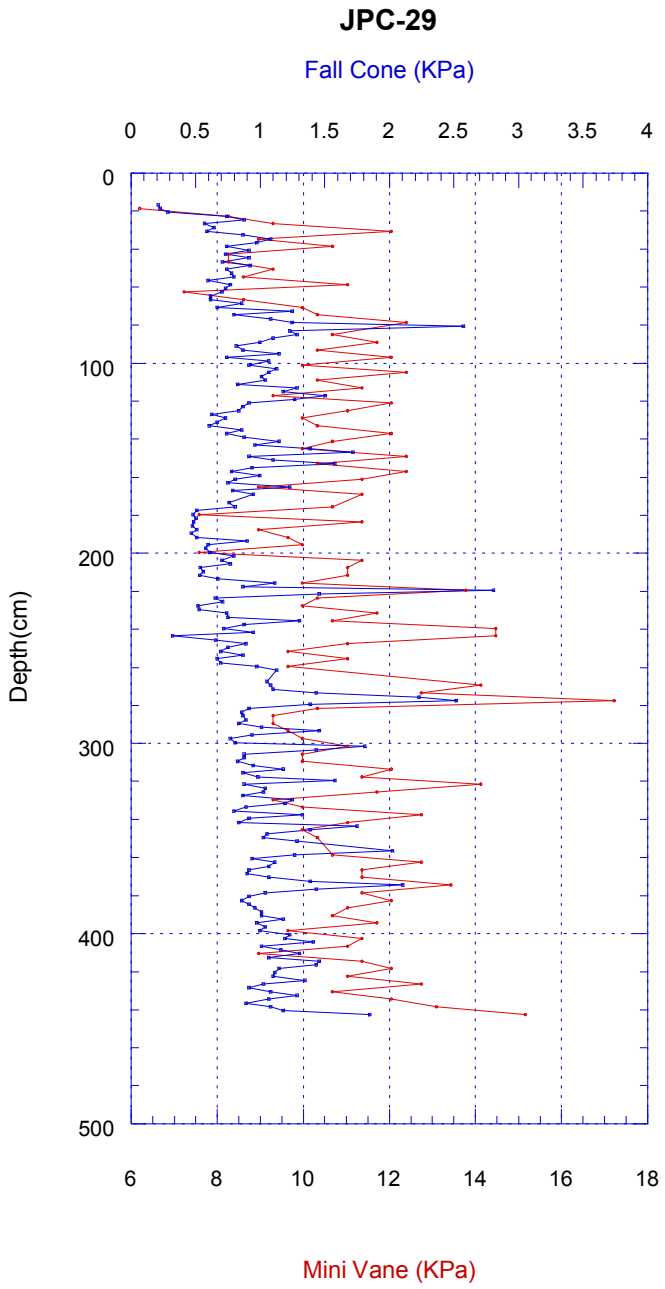

Figure 10 Comparison of shear strength profiles obtained by mini vane and fall cone tests for JPC-29.

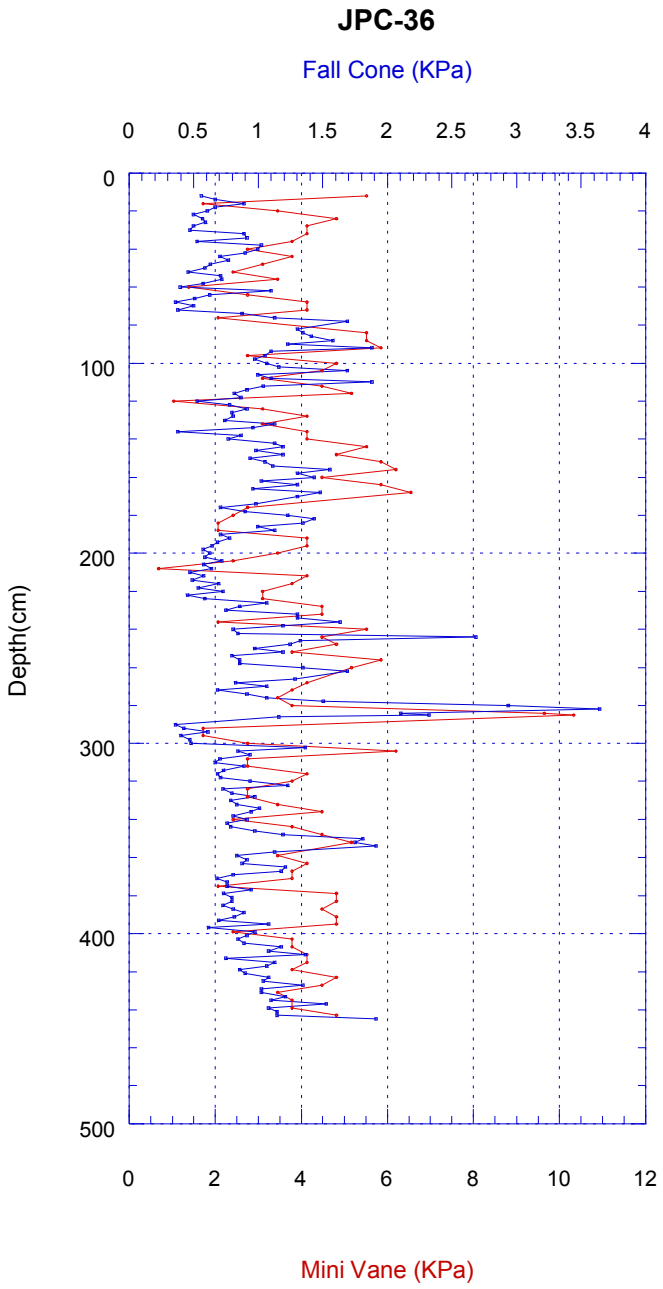

Figure 11 Comparison of shear strength profiles obtained by mini vane and fall cone tests for JPC-36.

The shear strength profiles have a very consistent behavior between cores; nevertheless, the mini vane test results for both cores are not in the same range. Shear strength in JPC-29 is approximately 6 kPa higher than JPC-36 along the whole profile. The mini vane method is very operator dependent (ASTM D4648-10); so the relatively constant difference between the profiles leads us to believe that the difference may be due to a subtle, systematic variation in operator technique.

The “calcium carbonate” content of the sediments was determined by using the coulometer to measure the carbon produced when the sample was exposed to acid then calculating based upon the 12 g to 100 g ratio between the masses of carbon and “calcium carbonate”. A relative measure of the “calcium carbonate” of the sediments was determined using the XRF technique. Figure 12 shows the profiles of “calcium carbonate” and relative amount of calcium versus depth in cores JPC-29 and JPC-36. The different types of profiles exhibit very similar patterns. While it is conceivable that “calcium carbonate” and some other sedimentary source of “calcium carbonate” could vary in essentially the same fashion with depth, the most geologically likely explanation for this similarity is that the predominant source of calcium in the sediments is “calcium carbonate”. The similarity of values obtained by both techniques suggests detailed estimates of the “calcium carbonate” of the mini basin sediments can be determined by using results from the more specific but time consuming coulometer technique to scale values obtained with the XRF technique.

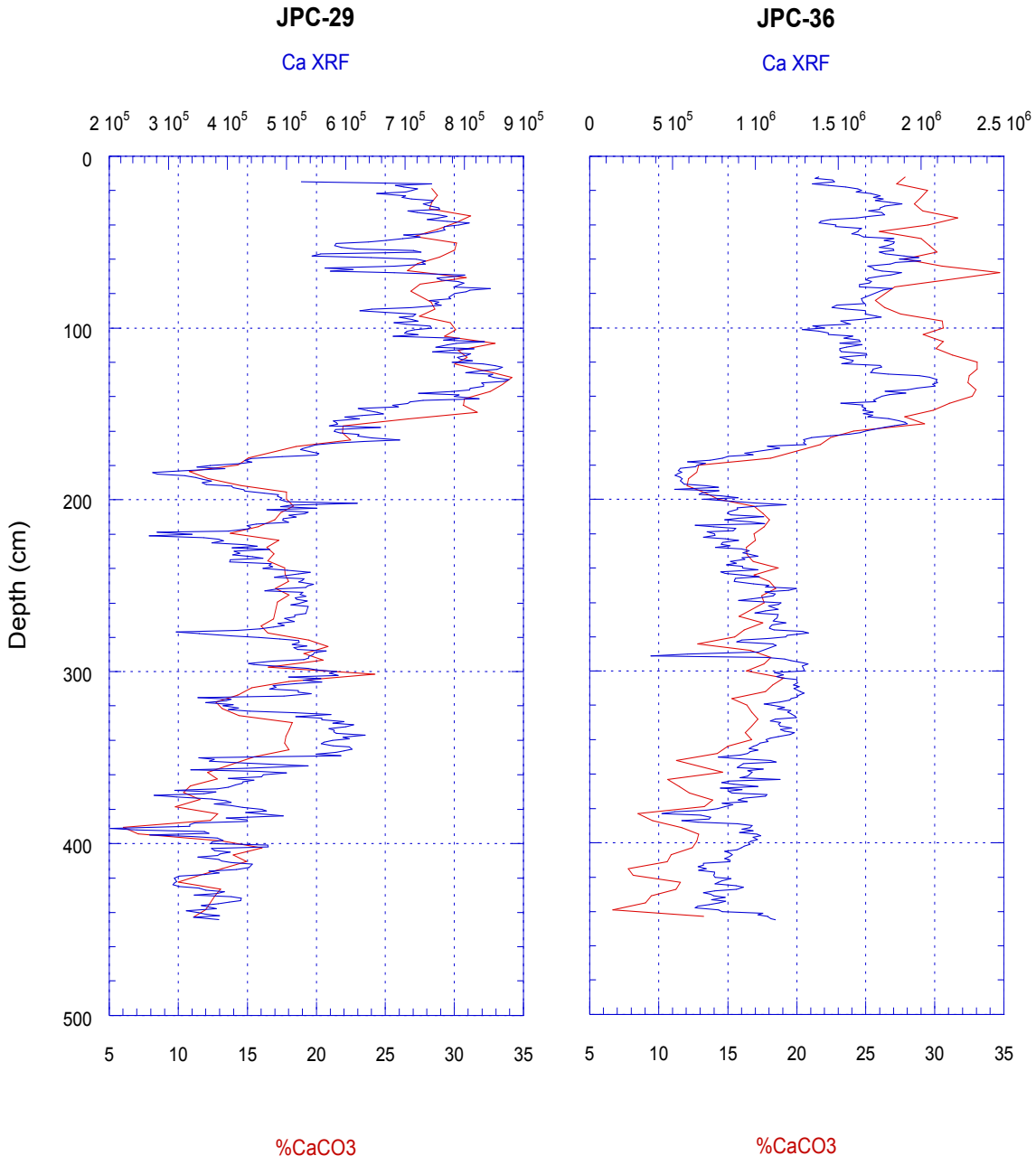

Figure 12 Profiles of “calcium carbonate” compared to the relative calcium content for core JPC-29 and JPC-36. The data obtained by the XRF replicates very well the data obtained by the coulometer.

4.3. Relationships Among Physical Properties

To better understand the variations of the physical properties with depth in the shallow seabed of the mini basin, it is compulsory to consider how the properties relate to each other.

Bulk density and water content are among the most fundamental sediment physical properties. The profiles of these two properties show an inverse relation (Figure 13); the layers of marine sediment with high bulk density correspond to low water content and vice versa. The plot of water content versus bulk density (Figure 14) shows that these two properties have an exponential inverse correlation with R=0.992 in JPC-29 and R=0.986 in JPC-36. A strong inverse relationship should exist in water saturated marine sediments because the sediment grains are several times denser than seawater (1.027 g/cm^3 for salinity of 35 ‰); therefore, the less water content in the sediment, the higher values of bulk density. That the bulk density and water content values correlate so closely implies that the density of the sediment grains is relatively constant (the 0.06 ± 2.64 g/cm^3 measured grain density confirms this) and attests to the veracity of the underlying laboratory measurements.

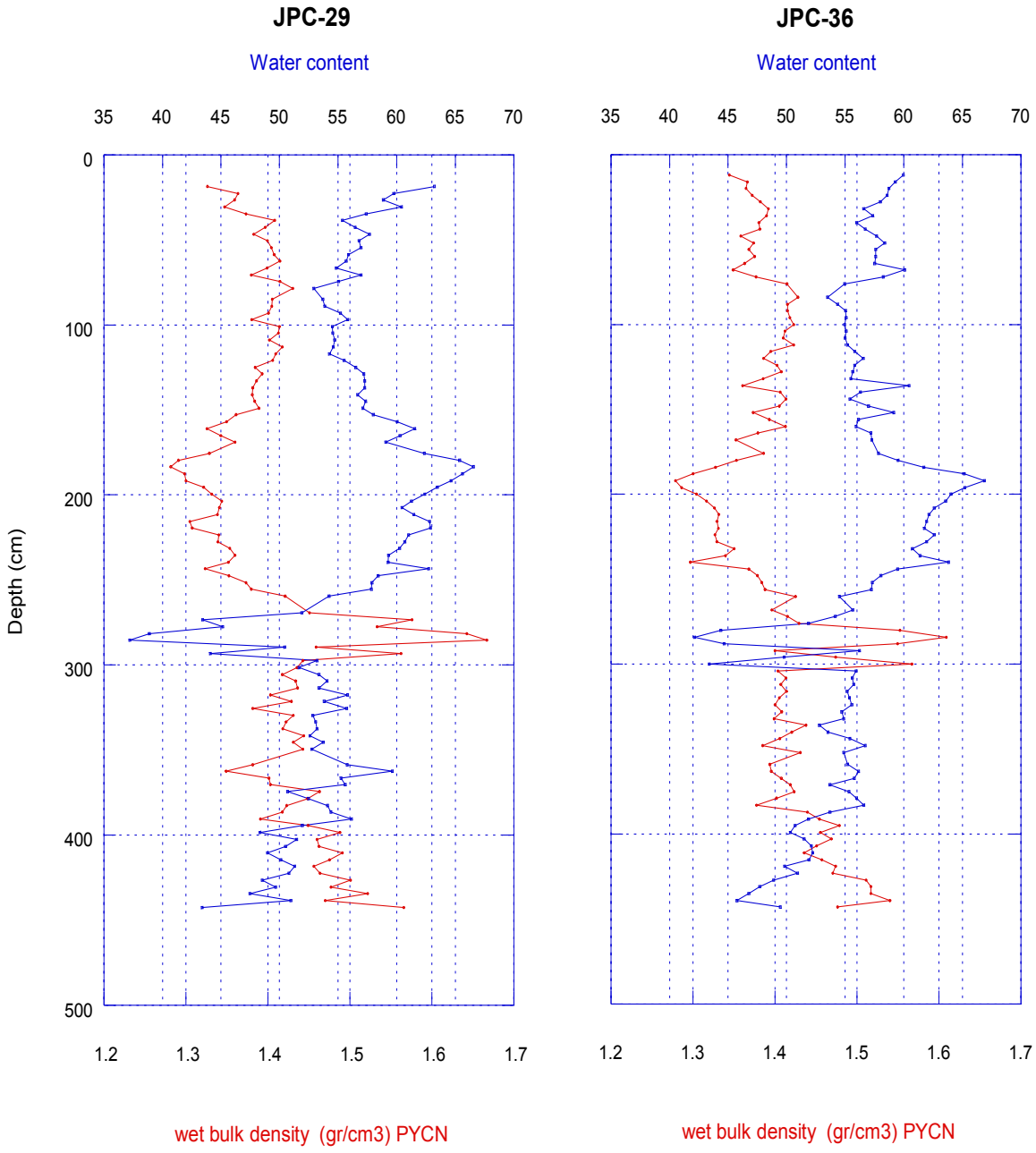

Figure 13 Profiles of bulk density and water content in JPC-29 and JPC-36.

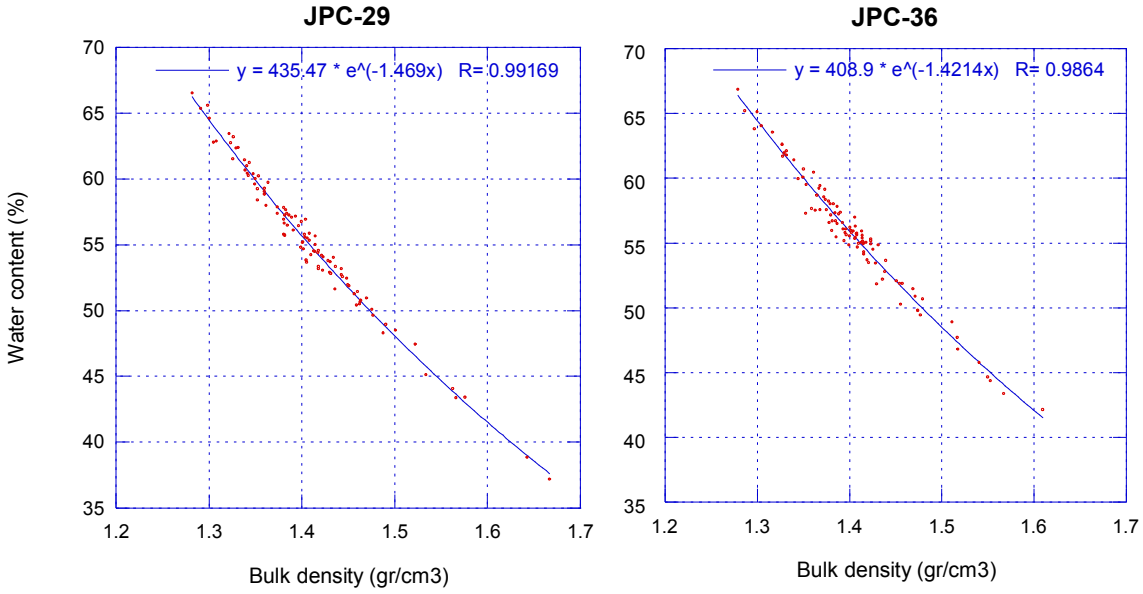

Figure 14 Plot of bulk density against water content in JPC-29 and JPC-36.

Significant changes in “calcium carbonate” content and bulk density occur between depth intervals A and B (Figure 15). The “calcium carbonate” content of the cores reaches a maximum value of over 30% between 0-150 cm depth and then falls to a minimum value of approximately 12% between 180-200 cm depth. Similarly, bulk density reaches a maximum value of 1.45 g/cm^3 between 0-150 cm depth and then falls to a relative minimum value of 1.31 g/cm^3 between 180-200 cm depth. Could the change in “calcium carbonate” content cause the change in density values?

“Calcium carbonate” has a grain density between 2.7 g/cm^3 and 2.9 g/cm^3 that is greater than other common marine sediment components (Schulz and Zabel., 2006). However, this grain density difference cannot be the cause of the bulk density maximum observed in the cores. Assuming that the “calcium carbonate” has a grain density of 2.75 g/cm^3, then the measured mean grain density of 2.65 g/cm^3 implies the other sediment components have a grain density of 2.625 g/cm^3. Given these values, the range in carbonate content from 12 to 30% would result in a change in the mean grain density of only 0.025 g/cm^3, which is less than 1% of the measured mean grain density of 2.65 g/cm^3. This variation in grain density is much too small to produce the observed 0.14 g/cm^3 (10.2%) change in bulk density.

A more likely explanation is that as the “calcium carbonate” content increases, the shapes and size distributions of the sediment grains change and hence the sediment’s fabric changes, resulting in a reduction in the pore space. Pore waters are displaced by sediment grains that have 2.65 times greater density and the bulk density of the sediments increases.

The spike in bulk density that occurs in the lower portion of interval B cannot be related to the influence of “calcium carbonate” because the “calcium carbonate” content is very low and relatively constant. Instead, the spike in bulk density corresponds directly to an increase in the size and size range of sediment grains. While the sediments in the cores are predominately clay sized with a presumably open, high-water content fabric, the spike in bulk density corresponds to a spike increase in the silt content from the background level of about 35 weight percent to about 60 weight percent (Ramirez and Slowey, unpublished). This change in grain size results in reduced pore volume and higher bulk density.

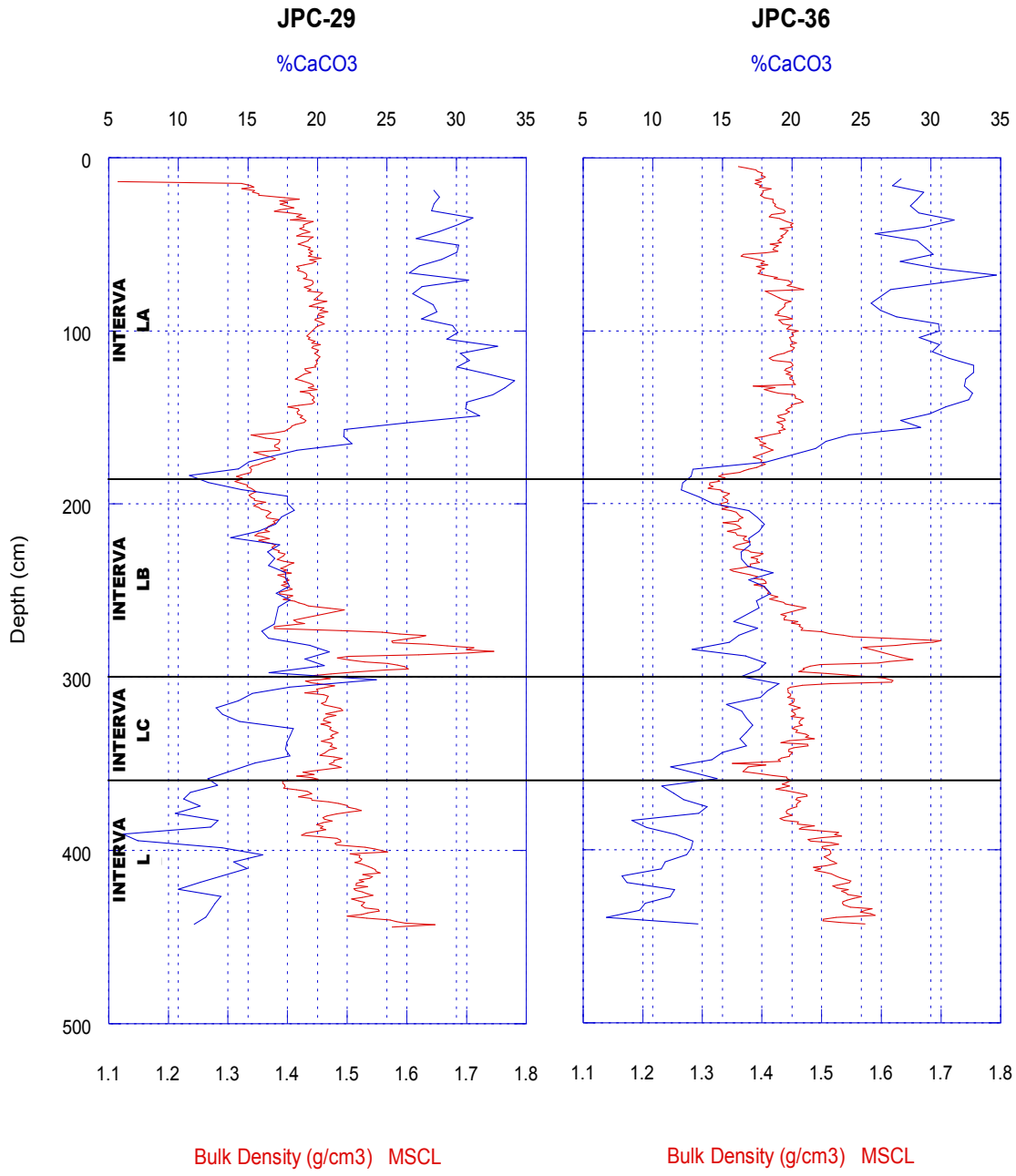

Figure 15 Comparison of bulk density profiles with “calcium carbonate” content for JPC-29 and JPC-36 with the intervals defined.

In both cores JPC-29 and JPC-36, the spike of high shear strength in the lower portion of depth interval B corresponds to sediment layers with high bulk density and low water content (Figure 16). As discussed above, the silt content of these sediment layers is nearly twice that of the adjacent sediments. These sediment layers also have the highest ratio of silica to aluminum measured in the cores. Siliclastic sediments normally have silica to aluminum ratios that vary between 11% and 14% and this range is apparent in cores JPC-29 and JPC-36 (Figure 17 and Figure 18). Those data points that deviate from this typical ratio of silica to aluminum indicate a greater abundance of silica, and correspond to the sediment layers with high shear strength and bulk density. The silica enrichment indicates the silt component of these sediment layers is comprised of quartz (which has Si but no Al). The decreased water content of these sediments, which leads to greater grain-to-grain contacts and so cohesion, and the more granular nature of the sediments both lead to the observed increase of shear strength.

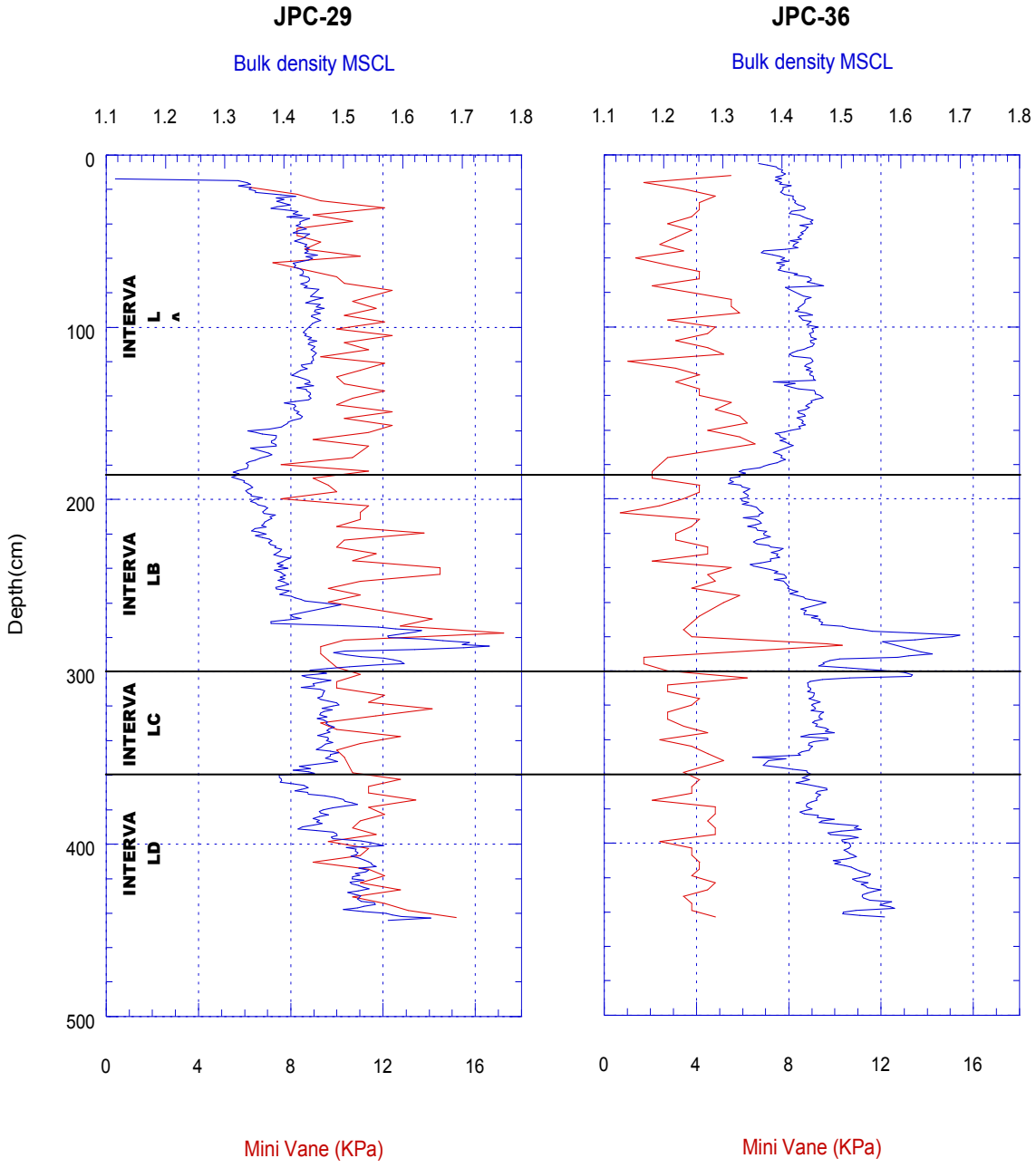

Figure 16 Comparison of shear strength profiles with bulk density profile for JPC-29 and JPC-36 with the intervals defined.

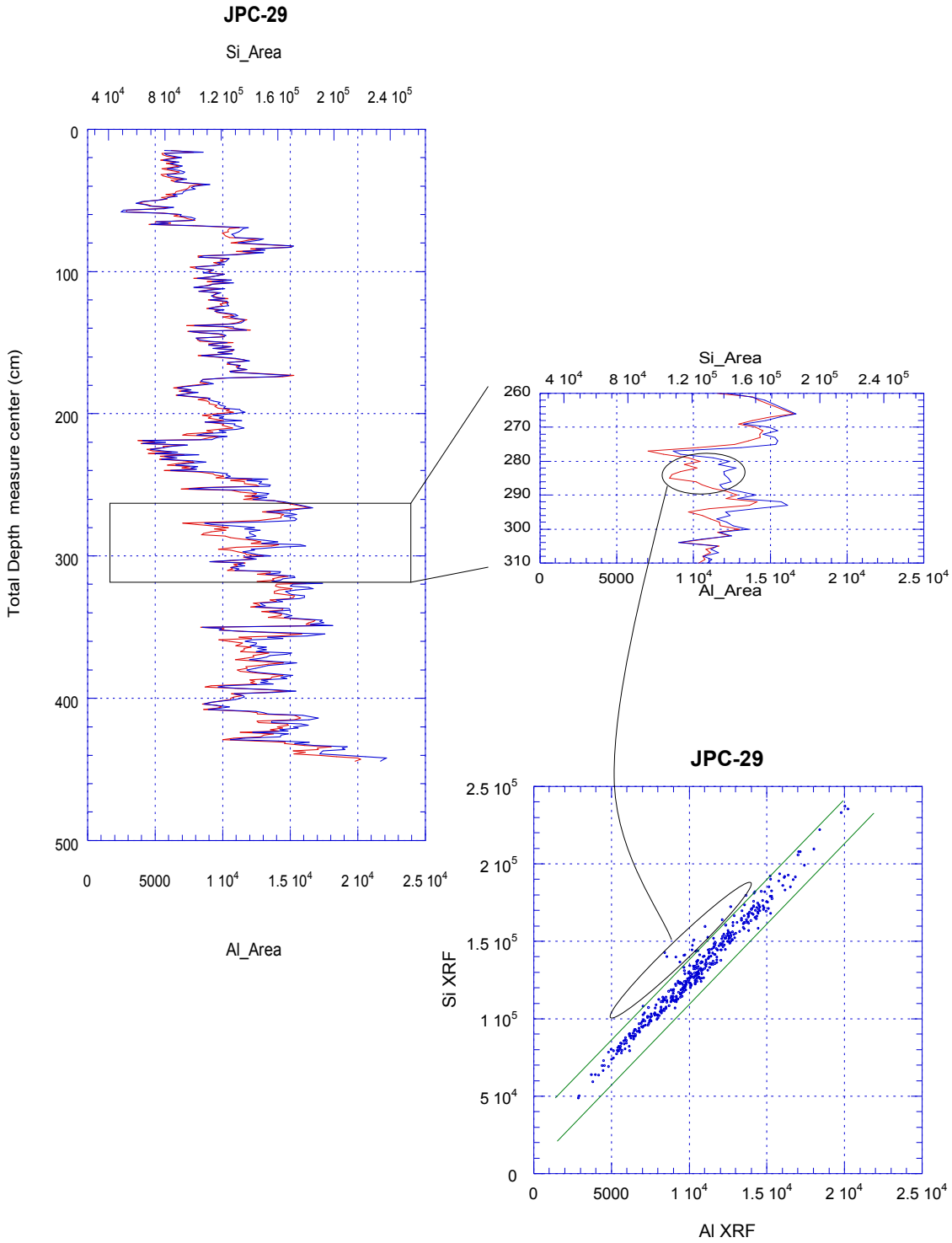

Figure 17 Profiles of Si and Al for JPC 29 show a close behavior along depth; the expanded view shows where the presence of silica is higher than aluminum. The plot of Si vs Al shows the values that do not fall along the expected trend and correspond to the depths where the profiles show higher silica presence.

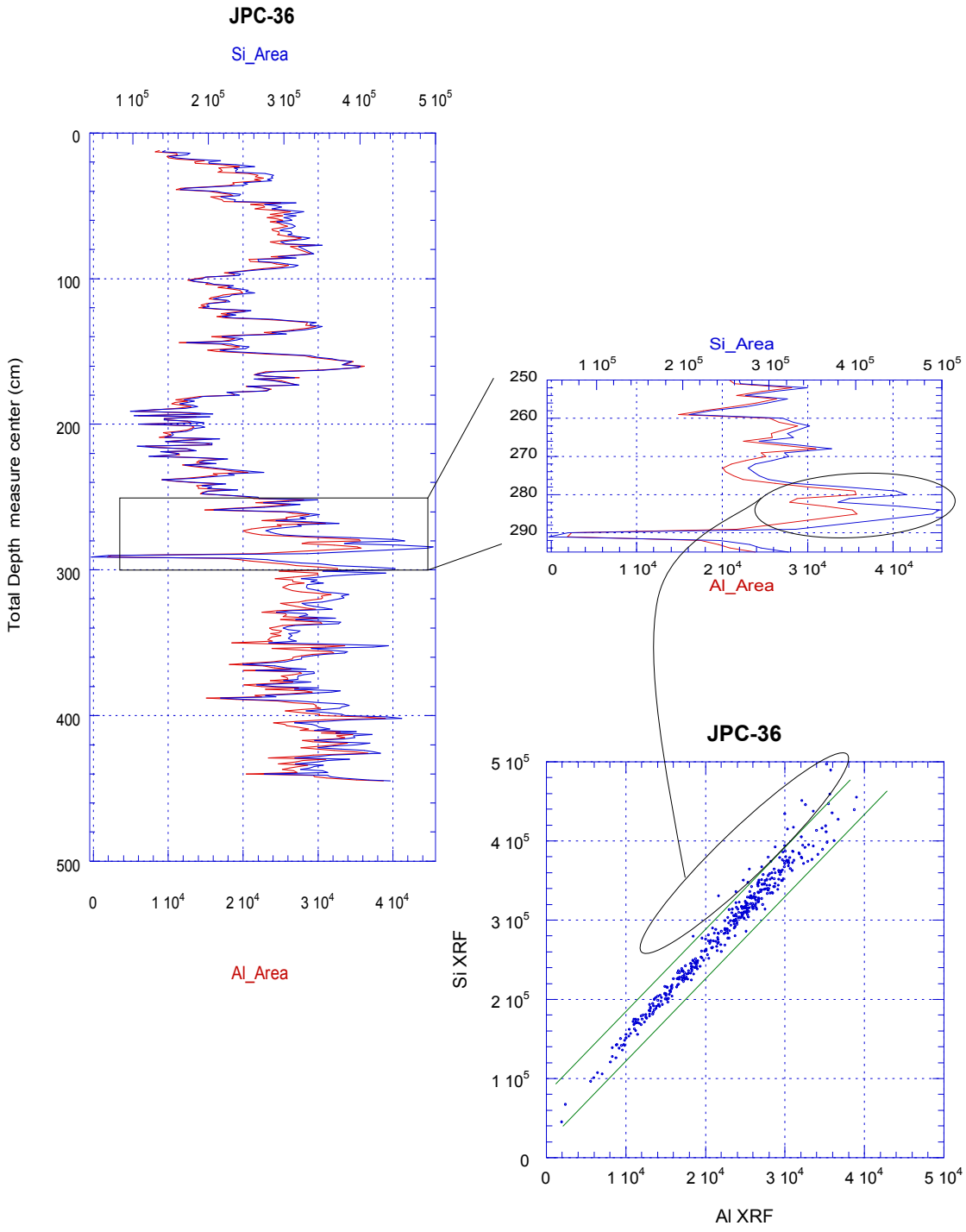

Figure 18 Profiles of Si and Al for JPC 36 show a close behavior along depth; the expanded view shows where the presence of silica is higher than aluminum. The plot of Si vs Al shows the values that do not fall along the expected trend and correspond to the depths where the profiles show higher silica presence.

This behavior of shear strength related to bulk density indicates that sediments with higher bulk density tend to show more shear strength. The shear strength depends on the contact and friction between sediment grains, thus to increase the shear strength is needed more grain contact and this happens when the sediments have higher bulk density.

4.4. Influence of Sampling Resolution

The depth interval at which measurements are made affects our ability to detect and resolve changes in sediment physical properties with depth in the seabed. Important data may be missed when the sampling resolution is too coarse, while time and financial resources may be used inefficiently when the sampling resolution is to fine. The very close intervals of measurements obtained during this study provide a unique opportunity to consider consequences of different sampling resolutions.

Figure 19 compares the bulk density profile obtained from core JPC-29 with a sampling resolution of 1 cm with profiles that would have been obtained with coarser sampling resolutions. As the sampling interval increases, the profile represents bulk density variations less accurately. For example, the profile with the sampling interval of 6 cm displays the overall shape of the original profile; however, some important features are not longer expressed as clearly (e.g., the spike of high density in the lower portion of depth interval B shows just two peaks instead of the original three).

The profiles of marine sediments physical properties presented by Silva et al. 2004, show a spike of high bulk density at about 2 m depth, which is consistent with a low spike in the water content profile at the same depth. However, the shear strength profile doesn't show any variation because the sampling resolution used was not sufficient to obtain to resolve it. Also, in the present research the importance of sampling resolution was noticed when the profile of "calcium carbonate" obtained by the coulometer, with a sampling resolution of 4 cm, wasn't able to resolve important features that the XRF did because its sampling resolution was 1 cm.

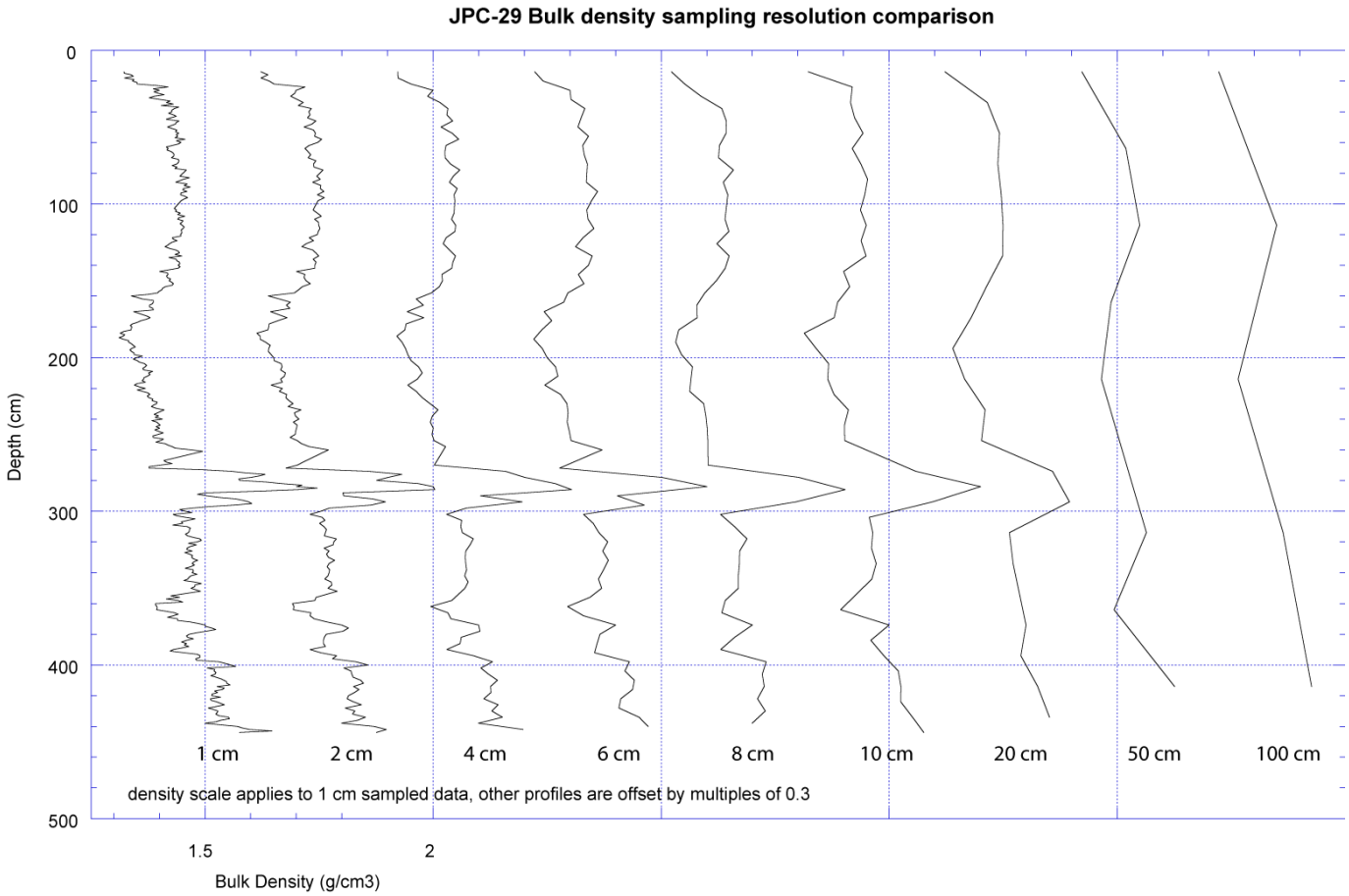

Figure 19 Comparison of the bulk density profiles with different sampling resolution.

5. SUMMARY AND CONCLUSIONS

A detailed investigation was made of the basic physical properties of two 5-m long cores of clayey marine sediments from a lower slope mini basin near Bryant and Keathley Canyons in the northwestern Gulf of Mexico. The results allow improved characterization of the shallow seabed of the lower slope and better understanding of the utility of several measurement techniques that may be used by geotechnical engineers and marine geologists to study marine sediments in many settings.

There is an overall trend of increasing bulk density with depth in the seabed, which is the expected result of normal consolidation of the sediments as they accumulate on the slope with the passage of time. The relationships among the sediment's physical properties clearly show that the changes in bulk density are mainly controlled by changes in water content – the grain density is relatively constant and the sediments are saturated with seawater, so the bulk density profile is a mirror image of the water content profile and an extremely high correlation exists between these two properties. Superimposed on the overall trend of increasing density with depth are two intervals of high density: the uppermost 0-180 cm of the seabed has relatively high density, carbonate rich sediments, and several closely spaced layers of coarser, high density, high shear strength sediments occur between 280-300 cm depth. In the upper high density interval, the higher "calcium carbonate" content influences density because "calcium carbonate" sediment grains are more closely packed than clay

mineral grains, but non-cohesive carbonate grains appear to have little effect on shear strength. The closely spaced layers that occur between 280-300 cm depth have both high bulk density and shear strength because they have a high content of quartz rich, silt size particles. The relatively wide range of grain sizes (clay and silt) and shapes (more rounded silt versus platey clay) results in decreased pore spaces and higher density. Greater shear strength results from the change in sediment fabric that leads to more grain to grain contacts and greater sediment cohesion, as well as the more granular nature of the silt.

Several sediment properties were each determined using independent techniques, providing an opportunity to consider the utility of these approaches. Determining sediment density using the MSCL was a very rapid and precise approach that yielded high resolution profiles. The bulk density values calculated using measured water content and grain density yielded values that compared very closely with those from the MSCL. Though a more tedious approach, it is more direct and provides an important validation of the MSCL results. Measures of sediment shear strength were obtained using both the motorized miniature vane and the fall cone techniques. Both techniques yielded similar overall profiles of shear strength. However, the results exhibited a relatively high degree of variability. As noted by the ASTM, simple determinations of shear strength are in general not very precise due to operator dependence and other factors. In this study, the apparent uncertainty of shear strength measurements is exacerbated by at least three factors. First, the total range of measured shear strengths is

small relative to the under certainty of the techniques. Also, the techniques actually measure different aspects and volumes of sediment. Visual inspection of the sediment cores and core photographs indicates that variations of sediment properties may occur on very fine spatial scales due to burrowing by organisms, the presence of small sedimentary structure, and other effects, so a portion of the variability among the measurements may actually represent true differences in the sediment properties that are typically not detected because the spatial resolution of shear strength measurements is relatively coarse. The chosen sampling interval influences how well measured profiles of sediment properties express actual variations in the seabed's characteristics, so the need to resolve seabed features must be balance by the practical availability of time and resources.

REFERENCES

Alves TM (2010) 3D seismic examples of differential compaction in mass-transport deposits and their effect on post-failure strata. Marine Geology 271:212-224. doi:10.1016/j.margeo.2010.02.014

American Society for Testing and Materials (ASTM) (2010) Standard test method for laboratory miniature vane shear test for saturated fine-grained clayey soil, D4648-10. Annual Book of ASTM Standards, Philadelphia. doi: 10.1520/D4648-10

American Society for Testing and Materials (ASTM) (2006) Standard test method for specific gravity of soils by gas pycnometer, D5550-06. Annual Book of ASTM Standards, Philadelphia. doi: 10.1520/D5550-06

Backman J, Moran K, McInroy DB, Mayer LA (2006) Expedition 302, Arctic Coring Expedition. Proceedings of the Integrated Ocean Drilling Program, 302:18-21

Baeten NJ, Laberg JS, Forwick M, Vorren TO, Ivanov M (2011) Small-scale mass wasting on the continental slope offshore Lofoten, northern Norway. Geophysical Research Abstracts 13:9771-9771

Booth JS (1979) Recent history of mass-wasting on the upper continental slope, northern Gulf of Mexico, as interpreted from the consolidation states of the sediment. Geology of Continental Slope 27:153-164

Bouma AH (1983) Intraslope basins in the Northwest Gulf of Mexico: a key to ancient submarine canyons and fans. AAPG Spec Pub 32:567-581

Boyce RE (1976) Definitions and laboratory techniques of compressional sound velocity parameters and wet-water content, wet bulk density, and porosity parameters by gravimetric and gamma ray attenuation techniques. Initial Reports of the Deep Sea Drilling Project, pp 931-951

Bradshaw AS, Silva AJ, Bryant WR (2000) Stress-strain and strength behavior of marine clays from continental slope, Gulf of Mexico. 14th Engineering Mechanics Conference, ASCE

Bryant WR, Bryant JR, Feeley MH, Simmons GR (1990) Physiographic and bathymetric characteristics of the continental slope, Northwest Gulf of Mexico. Geo-Marine Letters 10:182-199

Bryant WR, Simmons GR, Grim P (1991) The morphology and evolution of basins on the continental slope north-west Gulf of Mexico. Gulf Coast Association of Geological Societies Transactions 41:73-84

British Standard (BS) (1990) Test for soils for civil engineering purposes, BS 1377-2 Section 3.4 “Cone penetrometer method (definitive method)”, London. British Standards Institute

Combellas RI, Galoway WE (2006) Depositional and structural evolution of the middle Miocene depositional episode, east-central Gulf of Mexico. American Association of Petroleum Geologists Bulletin 90:335-362. doi: 10.1306/10040504132

Dadey KA, Janecek T, Klaus A (1992) Dry-bulk density: its use and determination. Proceedings of the Ocean Drilling Program, Scientific Results 126:551-554

Dezileau L, Pizarro C, Rubio M (2007) Sequential extraction of iron in marine sediments from the Chilean continental margin. Marine Geology 241:111-116. doi: 10.1016/j.margeo.2007.03.006

Duchamp-Alphonse S, Fiet N, Adatte T, Pagel M (2011) Climate and sea-level variations along the northwestern Tethyan margin during the Valanginian C-isotope excursion: Mineralogical evidence from the Vocontian Basin (SE France). Palaeogeography, Palaeoclimatology, Palaeoecology 302:243-254. doi:10.1016/j.palaeo.2011.01.015

Fairbanks RG (1989) A 17,000-year glacio-eustatic seal level record: influence of glacial melting rates on the Younger Dryas event and deep-ocean circulation. Nature 342:637-642

Francisca T, Yun TS, Ruppel C, Santamarina JC (2005) Geophysical and geotechnical properties of near-seafloor sediments in the northern Gulf of Mexico gas hydrate province. Earth and Planetary Science Letters 237:924-939.

Flower BP, Hastings DW, Hill HW, Quinn TM (2004) Phasing of deglacial warming and Laurentide ice sheet meltwater in the Gulf of Mexico. Geology 32:597-600

Finkl CW, Khalil SM, Andrews J, Keehn S, Benedet L (2006) Fluvial sand sources for barrier island restoration in Louisiana: geotechnical investigations in the Mississippi River. Journal of Coastal Research 22:773 – 787. doi: 10.2112/06A-0011.1

Gay A, Takano Y, Gilhooly WP, Berndt C, Heeschen K, Susuki N, Saegusa S, Nakagawa F, Tsunogai U, Jiang SY, Lopez M (2011) Geophysical and geochemical evidence of large scale fluid flow within shallow sediments in the eastern Gulf of Mexico, offshore Louisiana. Geofluids 11:34-47. doi: 10.1111/j.1468-8123.2010.00304.x

Hanor JS, Mercer JA (2009) Spatial variations in the salinity of pore waters in northern deep water Gulf of Mexico sediments: implications for pathways and mechanisms of solute transport. Geofluids 10:83-93. doi: 10.1111/j.1468-8123.2009.00271.x

Hasbro S (1957) A new approach to the determination of shear strength of clays by the fall cone test. Swedish Geotechnical Inst Proc No 14, Geotechnical Institute, Stockholm, pp 7-14

Holtz RD, Kovacs WD, Sheahan TC (2011) An introduction to geotechnical engineering, second edition. Pearson Education, Upper Saddle River, NJ, pp 523-552

Houlsby GT (1982) Theoretical analysis of fall cone test. Gëotechnique 32(2):111-118

Ingram WC, Meyers SR, Brunner CA, Martens CS (2010) Late Pleistocene–Holocene sedimentation surrounding an active seafloor gas-hydrate and cold-seep field on the Northern Gulf of Mexico Slope. Marine Geology 278:43-53. doi: 10.1016/j.margeo.2010.09.002

Kaiyu L (2009) Oxygen and carbon isotope analysis of the Mooreville Chalk and late Santonian-early Campanian sea level and surface temperature changes, northeastern Gulf of Mexico, USA. Cretaceous Research 30:980-990. doi: 10.1016/j.cretres.2009.02.008

Kastens, KA, Shor, AM (1985) Depositional processes of a meandering channel on Mississippi fan. American Association of Petroleum Geologists Bulletin 69:190-201

Kenter JAM, Schlager W (1989) A comparison of shear strength in calcareous and siliclastic marine sediments. Marine Geology 88:145-152

Keller GH, Bennett RH (1970) Variations in the mass physical properties of selected submarine sediments. Marine Geology 9:215-223. doi: 10.1016/0025-3227(70)90016-2

Kenyon NH (1987) Mass-wasting features on the continental slope of Northwest Europe. Marine Geology 74:57-77. doi: 10.1016/0025-3227(87)90005-3

Kilhams B, Godfrey S, Hartley A, Huuse M (2011) An integrated 3D seismic, petrophysical and analogue core study of the Mid-Eocene Grid channel complex in the greater Nelson Field area, UK Central North Sea. Geological Society of London 17:127-142. doi: 10.1144/1354-079310-022

Kim GY, Kim DC (2001) Comparison and correlation of physical properties from the plain and slope sediments in the Ulleung Basin, East Sea (Sea of Japan). Journal of Asian Earth Sciences 19:669-681

Knebes HJ, Carson B (1979) Small-scale slump deposits, Middle Atlantic Continental Slope, off eastern United States. Marine Geology 29:221-236. doi: 10.1016/0025-3227(79)90110-5

Konyukhov AI (2008) Geological structure, evolution stages, and petroliferous complexes of the Gulf of Mexico basin. Lithology and Mineral Resources 43:380-393. doi: 10.1134/S0024490208040081

Koumoto T, Houlsby GT (2001) Theory and practice of the fall cone test. Gëotechnique 51(8):701-712

Lee C, Yunb TS, Lee JS, Bahk JJ, Santamarina JC (2011) Geotechnical characterization of marine sediments in the Ulleung Basin, East Sea. Engineering Geology 117:151-158. doi: 10.1016/j.enggeo.2010.10.014

Lee GH, Watkins JS, Bryant WR (1996) Bryant Canyon fan system: an unconfined, large river sourced system in the Northwestern Gulf of Mexico. AAPG Bulletin 80(3):340-358

Lowrie A, Lutken CB, McGee TM (2004) Multiple outer shelf deltas and downslope massive mass-wastings characterize the Mississippi Canyon, Northern Gulf of Mexico. Gulf Coast Association of Geological Societies Transactions 54:383-392

Lu T, Bryant WR (1997) Comparison of vane shear and fall cone strengths of soft marine clay. Marine Georesources and Geotechnology 15:67-82

Mahiques MM, Fukumoto MM, Silveira IC Figueira RC, Bicego MC, Lourenço RA, Mello SH (2007) Sedimentary changes on the Southeastern Brazilian upper slope during the last 35,000 years. Anais Da Academia Brasileira de Ciencias 79:171-181

Mallarino G, Beaubouef RT, Droxler AW, Abreu V, Labeyrie L (2006) Sea level influence on the nature and timing of a minibasin sedimentary fill (northwestern slope of the Gulf of Mexico). American Association of Petroleum Geologists Bulletin 90:1089-1119. doi: 10.1306/02210605058

Meckler AN, Schubert CJ, Hochuli PA, Plessen B, Birgel D, Flower BP, Hinrichs KU, Haug GH (2008) Glacial to Holocene terrigenous organic matter input to sediments from Orca Basin, Gulf of Mexico — A combined optical and biomarker approach. Earth and Planetary Science Letters 272:251-263. doi: 10.1016/j.epsl.2008.04.046

Masson DG (1999) Sedimentary processes shaping the eastern slope of the Faeroe-Shetland Channel. Continental Shelf Research 21:825-857. doi: 10.1016/S0278-4343(00)00115-1

Moore D (1962) Bearing strength and other physical properties of some shallow and deep-sea sediments from the North Pacific. Geological Society of America Bulletin 13:1163-1166

Morton RA (2008) Historical Changes in the Mississippi-Alabama barrier-island chain and the roles of extreme storms, seal level, and human activities. Journal of Coastal Research 24:1587-1600, doi: 10.2112/07-0953.1

Posamentier HW, Walker RG (2006) Deep-Water turbidites and submarine fans. Facies Models Revisited 84:399-520

Richards AF, Keller GH (1967) Measurement of shear strength, bulk density and pore pressure in recent marine sediments by in situ probes: results of 1967 shallow-water tests. Bulletin of American Association of Petroleum Geologists 52:547-550

Rodrigues T, Grimalt JO, Abrantes F, Naughton F, Flores JA (2010) The last glacial–interglacial transition (LGIT) in the western mid-latitudes of the North Atlantic: Abrupt sea surface temperature change and sea level implications. Quaternary Science Reviews 29:1853-1862. doi: 10.1016/j.quascirev.2010.04004

Rothwell RG, Rack FR (2006) New techniques in sediment core analysis. Geological Society, London, Special Publications 267:1-29

Ryan WBF, Carbotte SM, Coplan JO, O'Hara S, Melkonian A, Arko R, Weissel RA, Ferrini V, Goodwilliwe A, Nitsche F, Bonczkowski J, Zemsky R (2009) Global Multi-Resolution Topography synthesis, Geochem Geophys Geosyst, 10, Q03014. doi: 10.1029/2008GC002332

Sager WW, MacDonald IR, Hou R (2003) Geophysical signatures of mud mounds at the hydrocarbon seeps on the Louisiana continental slope, northern Gulf of Mexico. Marine Geology 198:97-132. doi: 10.1016/S0025-3227(03)00097-5

Schlager W, Camber O (1986) Submarine slope angles, drowning unconformities, and self-erosion of limestone escarpments. Geological Society of America 14:762-765. doi: 10.1130/0091-7613

Schulz HD, Zabel M (2006) Marine Geochemestry. Springer-Verlag Berlin Heidelberg, New York, pp 318-321

Silva AJ, Baxter CDP, LaRosa PT, Bryant WR (2004) Investigation of mass wasting on the continental slope and rise. Marine Geology 203:355-366. doi: 10.1016/S0025-3227(03)00315-3

Skempton AW (1953) Soil mechanics in relation to geology. Yorkshire Geological Society 29:33-62

Takahashi K, Ravelo AC, Zarikian CA (2011) IODP Expedition 323-Pliocene and Pleistocene Paleoceanographic Changes in the Bering Sea. Scientific Drilling No 11. doi:10.2204/iodp.sd.11.01.2011

Tappin DR, McNiell LC, Henstock T, Mosher D (2010) Mass wasting processes – offshore Sumatra. Submarine mass movements and their consequences III, Springer, pp 327-336

Tripsanas EK, Bryant WR, Slowey NC, Bouma AH, Karageorgis AP, Berti D (2007) Sedimentological history of Bryant Canyon area, northwest Gulf of Mexico, during the last 135 kyr (Marine Isotope Stages 1-6): A proxy record of Mississippi River discharge. Palaeogeography, Palaeoclimatology, Palaeoecology 246:137-161. doi: 10.1016/j.palaeo.2006.10.032

Tripsanas EK, Bryant WR, Slowey NC, Kim JW (2006) Marine Isotope Stage 6 Canyon and spillover deposits of the Bryant and Eastern Canyon systems, northwest Gulf of Mexico: Importance of fine-grained turbidites on a delta fed prograding slope. Journal Sedimentary Research 23:44-48. doi: 10.2110/jsr.2006.083

Tripsanas EK (2003) Evolution of sedimentological and slope instability processes on the Bryant Canyon area, northwest Gulf of Mexico, Ph.D. Dissertation, Texas A&M University, College Station, pp 38-42

Twichell DC (2011) Review of recent depositional processes on the Mississippi fan, Eastern Gulf of Mexico. Gulf of Mexico origin, waters, and biota: vol 3, Geology, first edition. Texas A&M University press, College Station, TX. pp 141-154

Urgeles R, Locat J, Sawyer DE, Flemings PB, Dugan B, Binh NTT (2010) History of pore pressure build up and slope instability in mud-dominated sediments of Ursa Basin, Gulf of Mexico continental slope. Advances in Natural and Technological Hazards Research 28:179-190. doi: 10.1007/978-90-481-3071-9_15

Waelbroeck C, Labeyrie L, Michel E, Duplessy JC, McManus JF, Lambeck K, Balbon E, Labracherie M (2002) Sea-level and deep water temperature changes derived from benthic foraminifera isotopic records. Quaternary Science Reviews 21:295-305

Wood DM (1985) Some fall cone tests. Gëotechnique 35(1):64-68

VITA

Marco Antonio Santos Castaneda received his Bachelor of Science degree in naval sciences from University Comandante Rafael Moran Valverde, Ecuador in 2000. He joined the Ecuadorian Oceanographic Institute and won a scholarship to pursue a Master of Science degree in the Department of Oceanography at Texas A&M University.

Marco Antonio Santos Castaneda may be reached at Instituto Oceanografico de la Armada, Base Naval Sur, Guayaquil- Ecuador. His email is marcosantosc@hotmail.com